

RECEIVED: December 3, 2019

REVISED: February 13, 2020

ACCEPTED: February 16, 2020

PUBLISHED: March 6, 2020

Search for a heavy Higgs boson decaying to a pair of W bosons in proton-proton collisions at $\sqrt{s} = 13$ TeV



The CMS collaboration

E-mail: cms-publication-committee-chair@cern.ch

ABSTRACT: A search for a heavy Higgs boson in the mass range from 0.2 to 3.0 TeV, decaying to a pair of W bosons, is presented. The analysis is based on proton-proton collisions at $\sqrt{s} = 13$ TeV recorded by the CMS experiment at the LHC in 2016, corresponding to an integrated luminosity of 35.9 fb^{-1} . The W boson pair decays are reconstructed in the $2\ell 2\nu$ and $\ell\nu 2q$ final states (with $\ell = e$ or μ). Both gluon fusion and vector boson fusion production of the signal are considered. Interference effects between the signal and background are also taken into account. The observed data are consistent with the standard model (SM) expectation. Combined upper limits at 95% confidence level on the product of the cross section and branching fraction exclude a heavy Higgs boson with SM-like couplings and decays up to 1870 GeV. Exclusion limits are also set in the context of a number of two-Higgs-doublet model formulations, further reducing the allowed parameter space for SM extensions.

KEYWORDS: Hadron-Hadron scattering (experiments), Higgs physics

ARXIV EPRINT: [1912.01594](https://arxiv.org/abs/1912.01594)

Contents

1	Introduction	1
2	The CMS detector	3
3	Data and simulated samples	3
4	Event reconstruction	5
5	Signal models	7
6	Selection and categorization	9
6.1	$X \rightarrow 2\ell 2\nu$	9
6.1.1	Different-flavour final state	9
6.1.2	Same-flavour final state	10
6.2	$X \rightarrow \ell\nu 2q$	10
6.2.1	Boosted final state	12
6.2.2	Resolved final state	12
7	Background estimation	12
7.1	$X \rightarrow 2\ell 2\nu$	14
7.2	$X \rightarrow 2\nu 2q$	16
8	Signal extraction and systematic uncertainties	16
8.1	$X \rightarrow 2\ell 2\nu$	19
8.2	$X \rightarrow \ell\nu 2q$	19
9	Results	19
10	Summary	22
	The CMS collaboration	34

1 Introduction

The discovery of the standard model (SM) Higgs boson, with a mass close to 125 GeV, by the CERN LHC experiments ATLAS and CMS in 2012 [1–3] represents a major advancement in particle physics. Studies of the new particle have so far shown consistency with the SM Higgs mechanism predictions [4–15]. Throughout this paper, the observed SM Higgs boson is denoted as h(125). In order to determine whether the SM gives a complete description of the Higgs sector, precise measurements of the h(125) coupling strengths,

CP structure and kinematic distributions are required [16–20]. A complementary strategy involves the search for an additional Higgs boson, denoted X, whose existence would prove the presence of beyond the SM (BSM) physics in the form of a non minimal Higgs sector [21, 22]. The search for an additional scalar resonance in the full mass range accessible at the LHC remains one of the main objectives of the experimental community.

The search for a high-mass Higgs boson has been performed at ATLAS [23–26] and CMS [27, 28] in a number of final states, using proton-proton (pp) collisions at centre-of-mass energies (\sqrt{s}) of 7, 8 and 13 TeV, with no significant excess observed. For Higgs boson masses above 200 GeV one of the most sensitive channels is the decay to a pair of W bosons [22]. In this analysis, a search is performed in the fully leptonic, $2\ell 2\nu$, and semileptonic, $\ell\nu 2q$, WW decay channels (with $\ell = e$ or μ) using pp collisions recorded at $\sqrt{s} = 13$ TeV by the CMS experiment in 2016, corresponding to an integrated luminosity of 35.9 fb^{-1} .

The fully leptonic channel has a clear signature of two isolated leptons and missing transverse momentum (p_T^{miss}), due to the neutrinos escaping detection. For the semileptonic channel, the leptonically decaying boson is reconstructed as a single isolated lepton and p_T^{miss} . The hadronically decaying boson may be sufficiently boosted that its decay products are contained in a single merged jet. Jet substructure techniques are used to identify merged jets with two well defined subjets and to determine the merged jet mass, helping to discriminate vector boson hadronic decays from other jets. When the W boson hadronic decay products are resolved, it may be reconstructed using two quark jets (a dijet). The search is performed in a wide mass range from 0.2 up to 3.0 TeV. Events are categorized to enhance the sensitivity to the gluon fusion (ggF) and vector boson fusion (VBF) Higgs boson production mechanisms.

A signal interpretation in terms of a heavy Higgs boson with SM-like couplings and decays is performed. This is motivated by BSM models in which the $h(125)$ mixes with a heavy electroweak singlet, resulting in an additional resonance at high-mass with couplings similar to those of the SM Higgs boson [21]. The signal model includes a detailed simulation of the interference between the X signal, the $h(125)$ off-shell tail, and the WW background [29]. A number of hypotheses for the relative contribution of ggF and VBF production are investigated.

Additional interpretations based on a number of two-Higgs-doublet models (2HDMs) [22] are performed. The 2HDM, which introduces a second scalar doublet, is incorporated in supersymmetric [30] and axion [31] models, and may introduce additional sources of explicit or spontaneous CP violation that could explain the baryon asymmetry of the Universe [32]. As will be discussed in section 5, the measured properties of the $h(125)$ set strong constraints on the decay of a heavy Higgs boson to vector bosons in the context of 2HDMs.

This paper is organized as follows: in section 2, a brief description of the CMS detector is provided; section 3 gives a description of the data and Monte Carlo (MC) simulated samples used in the analysis; section 4 provides a description of the event reconstruction; section 5 contains an overview of the signal models considered; in section 6, the event selection and categorization are discussed; section 7 explains the estimation of the SM backgrounds; the signal extraction procedure and the systematic uncertainties affecting

the analysis are presented in section 8; the results are presented in section 9. Finally, results are summarized in section 10.

2 The CMS detector

The CMS detector, described in detail in ref. [33], is a multipurpose apparatus designed to study high transverse momentum (p_T) physics processes in pp and heavy-ion collisions. A superconducting solenoid occupies its central region, providing a magnetic field of 3.8 T parallel to the beam direction. Charged-particle trajectories are measured by the silicon pixel and strip trackers, which cover a pseudorapidity region of $|\eta| < 2.5$. A crystal electromagnetic calorimeter (ECAL), and a brass and scintillator hadron calorimeter surround the tracking volume and cover $|\eta| < 3$. The steel and quartz-fiber Cherenkov hadron forward (HF) calorimeter extends the coverage to $|\eta| < 5$. The muon system consists of gas-ionization detectors embedded in the steel flux return yoke outside the solenoid, and covers $|\eta| < 2.4$. The first level of the CMS trigger system [34], composed of custom hardware processors, is designed to select the most interesting events in less than 4 μ s, using information from the calorimeters and muon detectors. The high-level trigger processor farm further reduces the event rate to 1 kHz before data storage.

3 Data and simulated samples

The events used to study the $\ell\nu 2q$ final state are selected by high-level trigger algorithms that require the presence of one electron with $p_T > 25$ GeV and $|\eta| < 2.1$ passing tight identification and isolation requirements, or one muon with $p_T > 24$ GeV and $|\eta| < 2.4$ passing loose identification and isolation requirements. The trigger efficiency for $\ell\nu 2q$ signal events passing the offline event selection is about 93%. Both single-lepton and dilepton triggers are used to select events to study the $2\ell 2\nu$ final state. In addition to the single-lepton triggers described, the $2\ell 2\nu$ final state events are also selected by a trigger which requires one electron outside the central region ($2.1 < |\eta| < 2.5$) with $p_T > 27$ GeV. The dilepton triggers require the presence of two leptons passing relatively loose identification and isolation requirements. For the dielectron (dimuon) trigger, the p_T thresholds are 23 (17) GeV for the leading and 12 (8) GeV for the subleading electrons (muons). For the different-flavour dilepton trigger, the p_T thresholds are either 8 GeV for the muon and 23 GeV for the electron, or 23 GeV for the muon and 12 GeV for the electron. The overall trigger efficiency for the combination of the single-lepton and dilepton triggers for $2\ell 2\nu$ signal events passing the offline event selection is larger than 99%.

Several event generators are used to optimize the analysis and estimate the yields of signal and background events, as well as the associated systematic uncertainties. The heavy Higgs boson signal samples are generated in the ggF and VBF production modes at next-to-leading order (NLO) in quantum chromodynamics (QCD) using POWHEG v2 [35–39], for a number of masses ranging from 0.2 to 3.0 TeV. The resonance width is set according to the SM Higgs boson expectation for signal masses up to 1 TeV. For signal masses higher than 1 TeV the width is set to half the resonance mass, which approximately corresponds

to the SM Higgs boson prediction at 1 TeV. The decay of the signal to a pair of W bosons is simulated with JHUGEN v6.2.8 [40, 41]. The simulated signal samples are normalized using cross sections and decay rates computed by the LHC Higgs Cross Section Working Group [42].

The W+jets process is produced at NLO with the MADGRAPH5_aMC@NLO v2.2.2 event generator [43], using the FxFx merging scheme [44] between the jets from matrix element calculations and parton showers (PS), and scaled to the next-to-NLO (NNLO) cross section computed using FEWZ v3.1 [45].

Single top quark and $t\bar{t}$ processes are generated at NLO using POWHEG [46, 47] and MADGRAPH5_aMC@NLO. The cross sections of the different single top quark processes are calculated at NLO [48], while the $t\bar{t}$ cross section is computed at NNLO, with next-to-next-to-leading-logarithmic soft-gluon resummation [49].

The WW diboson continuum background is simulated in a number of ways. The production of WW via $q\bar{q}$ ($q\bar{q} \rightarrow WW$) is generated using POWHEG [50] and MADGRAPH5_aMC@NLO at NLO, WW production via gluon fusion ($gg \rightarrow WW$) is generated using MCFM v7.0 [51] at leading order (LO), while a WW plus two jets ($qq \rightarrow qqWW$) sample is produced with MADGRAPH5_aMC@NLO at LO. The cross section used for normalizing the WW processes produced via $q\bar{q}$ is computed at NNLO [52]. For the $gg \rightarrow WW$ process, the difference between LO and NLO cross sections is large; a scale factor of 1.4 is theoretically calculated [53] and applied to the cross section prediction from MCFM. In order to suppress the top quark background processes, the $2\ell 2\nu$ analysis implements an event categorization based on jet multiplicity. This approach spoils the convergence of fixed-order calculations of the $q\bar{q} \rightarrow WW$ process and requires the use of dedicated resummation techniques for an accurate prediction of the differential distributions [54, 55]. The simulated $q\bar{q} \rightarrow WW$ events are therefore reweighted to reproduce the p_T^{WW} distribution from the p_T -resummed calculation.

Drell-Yan (DY) production of Z/γ^* is generated at NLO using MADGRAPH5_aMC@NLO and scaled to the NNLO cross section computed using FEWZ. Multiboson processes such as WZ, ZZ, and VVV ($V = W, Z$) are also simulated at NLO with MADGRAPH5_aMC@NLO.

The QCD multijet production background is generated with PYTHIA 8.212 [56]. The QCD samples are enriched in events containing electrons or muons with dedicated filters.

All processes are generated using the NNPDF 3.0 [57, 58] parton distribution functions (PDFs), with the order matching that of the matrix element calculations. All the event generators are interfaced with PYTHIA for showering of partons and hadronization, and to simulate the underlying event (UE) and multiple-parton interactions based on the CUET8PM1 tune (CUETP8M2T4 for $t\bar{t}$ samples) [59]. To estimate systematic uncertainties related to the choice of UE and multiple-parton interactions tune, WW background samples are generated with two alternative tunes, which are representative of the uncertainties in the tuning parameters. A systematic uncertainty associated with showering and hadronization is estimated by interfacing the same samples with the HERWIG++ 2.7 generator [60, 61], using the UE-EE-5C tune for the simulation of UE and multiple-parton interactions [59].

For all processes, the detector response is simulated using a detailed description of the CMS detector, based on the GEANT4 package [62]. Additional pp interactions simulated with PYTHIA are overlaid on the event of interest to reproduce the number of interactions occurring simultaneously within the same bunch crossing (pileup) measured in data.

4 Event reconstruction

The particle-flow (PF) algorithm [63] is used to reconstruct the observable particles in the event. Clusters of energy deposits measured by the calorimeters, charged particle tracks identified in the central tracking system, and the muon detectors, are combined to reconstruct individual particles (PF candidates).

If more than one vertex is reconstructed, the vertex with the largest value of summed physics-object p_T^2 is taken to be the primary pp interaction vertex. The physics objects are those returned by a jet finding algorithm [64, 65] applied to all charged tracks assigned to the vertex, and the associated missing transverse momentum, computed as the negative vectorial sum of the p_T of those jets.

Electrons are reconstructed from a combination of the deposited energy of the ECAL clusters associated with the track reconstructed from the measurements determined by the inner tracker, and the energy sum of all photons spatially compatible with being bremsstrahlung from the electron track [66]. The electron candidates are required to have $|\eta| < 2.5$. Additional requirements are applied to reject electrons originating from photon conversions in the tracker material or jets mis-reconstructed as electrons. Electron identification criteria rely on observables sensitive to the bremsstrahlung along the electron trajectory, the geometrical and momentum-energy matching between the electron trajectory and the associated supercluster, as well as ECAL shower shape observables and compatibility with the primary vertex.

Muon candidates are reconstructed by combining charged tracks in the muon detector with tracks reconstructed in the central tracking system [67]. They are required to have $|\eta| < 2.4$. Identification criteria based on the number of hits in the tracker and muon systems, the fit quality of the muon track, and the consistency of the trajectory with the primary vertex, are imposed on the muon candidates to reduce the misidentification rate.

Prompt leptons from electroweak interactions are usually isolated, whereas misidentified leptons and leptons from jets, are often accompanied by charged or neutral particles, and can arise from a secondary vertex. Therefore leptons are required to be isolated from hadronic activity by requiring that the sum of the p_T of charged hadrons associated with the primary vertex, and the p_T of neutral hadrons and photons, in a cone around the lepton of radius $\Delta R = \sqrt{(\Delta\phi)^2 + (\Delta\eta)^2} = 0.4$ (where ϕ is the azimuthal angle in radians), is below a certain fraction of the lepton p_T . To mitigate the effect of pileup on the isolation variable, a correction based on the mean event energy density [68] is applied.

The jet reconstruction uses all PF candidates, except those charged candidates that are not associated with the primary vertex. This requirement mitigates the effect of pileup for $|\eta| < 2.5$. Particle candidates are clustered using the anti- k_T algorithm [64, 65] with a distance parameter of 0.4 (AK4) or 0.8 (AK8). To reduce the residual pileup contamination

from neutral PF candidates, a correction based on jet median area subtraction [68] is applied. The jet energy is calibrated using both simulation and data following the technique described in [69]. Only AK4 jets with $p_T > 30$ GeV (20 GeV for b quark jets) and $|\eta| < 4.7$ (2.4 for b quark jets) are considered. The AK8 jets are required to have $p_T > 200$ GeV and $|\eta| < 2.4$. Those AK4 (AK8) jets which overlap with a well identified and isolated lepton within a distance of $\Delta R = 0.4$ (0.8) are ignored.

The vector \vec{p}_T^{miss} , whose magnitude is the p_T^{miss} in the event, is computed as the negative vectorial sum in the transverse plane of all the PF candidates momenta. The \vec{p}_T^{miss} is modified to account for the corrections to the energy scale of the jets described above.

A jet grooming procedure, which removes contributions from soft radiation and additional interactions, is used on the AK8 jets to help identify and discriminate between jets from Lorentz-boosted hadronic W boson decays and jets from quarks and gluons. First, the pileup mitigation corrections provided by the pileup per particle identification (PUPPI) algorithm [70] are applied. The jets are then groomed by means of a modified mass drop algorithm [71, 72], known as the soft-drop algorithm [73], with parameters $\beta = 0$, $z_{\text{cut}} = 0.1$ and $R_0 = 0.8$. The soft-drop mass (m_J) used in the $\ell\nu 2q$ analysis is computed from the sum of the four-momenta of the jet constituents passing the grooming algorithm.

Discrimination between AK8 jets originating from W boson decays and those originating from gluons and quarks is also achieved by using the N -subjettiness jet substructure variable [74]. This observable exploits the distribution of the jet constituents found in the proximity of the subjet axes to determine if the jet can be effectively subdivided into a number N of subjets. The generic N -subjettiness variable τ_N is defined using the p_T -weighted sum of the angular distance $\Delta R_{N,k}$ of the jet constituents k with respect to the axis of the N^{th} subjet:

$$\tau_N = \frac{1}{d_0} \sum_k p_{T,k} \min(\Delta R_{1,k}, \Delta R_{2,k}, \dots, \Delta R_{N,k}). \quad (4.1)$$

The normalization factor d_0 is defined as $d_0 = \sum_k p_{T,k} R_0$, with R_0 being the clustering parameter of the original jet. The variable which best discriminates W boson jets from those coming from quarks and gluons is the ratio of the 2- to 1-subjettiness: $\tau_{21} = \tau_2/\tau_1$. The τ_{21} observable is calculated for the jet after applying the PUPPI algorithm corrections for pileup mitigation.

To identify jets coming from b quarks, a multivariate b tagging algorithm [75] and the combined secondary vertex algorithm [75] are used in the $2\ell 2\nu$ and $\ell\nu 2q$ analyses, respectively. In both cases, the chosen working point corresponds to about 80% efficiency for genuine b quark jets and to a mistagging rate of about 10% for light-flavour or gluon jets, and of about 40% for c quark jets.

For each event in the fully leptonic channel, at least two high- p_T lepton candidates originating from the primary vertex are required. Opposite-charge dielectron pairs, dimuon pairs and electron-muon ($e\mu$) pairs are accepted. In the semileptonic channel, at least one high- p_T lepton candidate, and two AK4 jets or one AK8 jet, originating from the primary vertex are required.

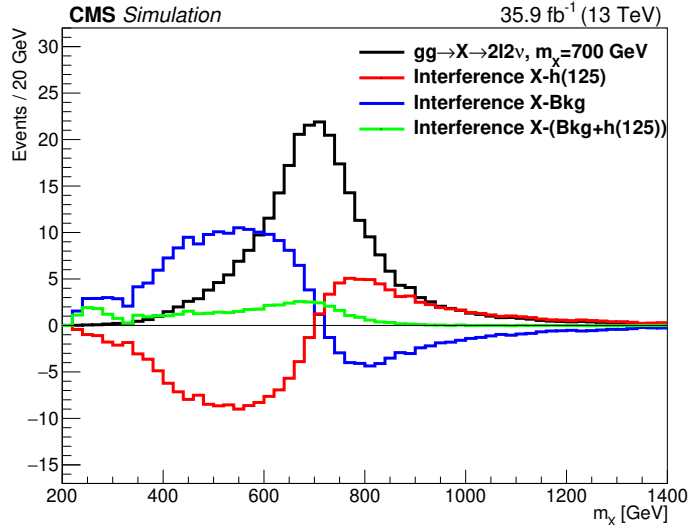


Figure 1. Generator-level mass of a ggF-produced 700 GeV signal (black line) normalized to the SM cross section and without considering interference effects. The effects of the interference of the signal with the $gg \rightarrow WW$ continuum and the $gg \rightarrow h(125)$ off-shell tail are shown, together with the total interference effect.

5 Signal models

A signal interpretation in terms of a heavy Higgs boson with SM-like couplings and decays is implemented in this analysis. Both the ggF and VBF production mechanisms are considered. Due to the large expected width of the X resonance at high-mass, its interference with the WW continuum and the $h(125)$ off-shell tail becomes significant [29]. The MELA matrix-element package [18, 40, 41], based on JHUGEN for Higgs bosons, and on MCFM for the continuum WW background, has been used to estimate the interference of high-mass X resonances with the WW continuum and the $h(125)$. The two sources of interference have opposite signs and partially cancel out with the size of the cancellation depending on the signal mass. Figure 1 displays the generator-level mass distribution of a ggF-produced 700 GeV signal and the effects of interference with the $gg \rightarrow WW$ continuum and $gg \rightarrow h(125)$ off-shell tail. The interference effect is taken into account for both the ggF and VBF production mechanisms. A parameter f_{VBF} , which is the fraction of the VBF production cross section with respect to the total cross section, is included in the model and a number of hypotheses investigated.

An interpretation in the context of a general 2HDM is conducted. Various formulations of the 2HDM predict different couplings of the two doublets to right-handed quarks and charged leptons: in the Type-I formulation [22], all fermions couple to only one Higgs doublet; in the Type-II formulation [22], the up-type quarks couple to a different doublet than the down-type quarks and leptons. There are five physical Higgs bosons predicted: two CP-even neutral bosons h and H ; a neutral CP-odd boson A ; and two charged bosons H^\pm . In most formulations of the 2HDM, h corresponds to the $h(125)$, and H is an additional high-mass CP-even Higgs boson. The 2HDM has two important free parameters, α and

$\tan\beta$, which are the mixing angle and the ratio of the vacuum expectation values of the two Higgs doublets, respectively. The quantity $\cos(\beta - \alpha)$ is also of interest, as the coupling of the heavy Higgs boson H to two vector bosons is proportional to this factor. In the alignment limit, which occurs at $\cos(\beta - \alpha) = 0$, the properties of h approach those of the SM Higgs boson, while the decay of H to vector bosons becomes heavily suppressed. Based on the constraints given by the measurements of the $h(125)$ couplings, the largest possible deviations of $\cos(\beta - \alpha)$ from 0 allowed are approximately 0.3 and 0.1 for the Type-I and -II scenarios respectively [76, 77]. Therefore the value of $\cos(\beta - \alpha)$ has been fixed to 0.1 for the 2HDM scenarios considered here. In this way the measured properties of the $h(125)$ are incorporated into the definition of the scenarios while still allowing for a non-negligible branching fraction for H to vector bosons. In the limit that $m_A \gg m_Z$, the masses of the H , A , and H^\pm bosons become approximately degenerate. For simplicity it is assumed that $m_H = m_A = m_{H^\pm}$ for the 2HDM scenarios considered. The width of H has a dependence on $\tan\beta$, with relatively large widths predicted in comparison to both the SM widths and the experimental resolution for $\tan\beta$ below ≈ 0.2 and m_H above ≈ 400 GeV. However, for the majority of the phase space explored the SM width assumption gives a reasonable approximation of the 2HDM predictions.

The minimal supersymmetric standard model (MSSM) [78, 79], which incorporates a Type-II 2HDM, is also considered. At tree level, the whole phenomenology can be described using just two parameters. By convention, these parameters are chosen to be $\tan\beta$ and m_A , the mass of the pseudoscalar Higgs boson. Beyond the tree level, the MSSM Higgs sector depends on additional parameters which enter via higher-order corrections in perturbation theory, and which are usually fixed to values motivated by experimental constraints and theoretical assumptions. The $m_h^{\text{mod}+}$ [80] and hMSSM [81–84] benchmark scenarios are defined by setting these parameters such that a wide range of the m_A - $\tan\beta$ parameter space is compatible with the $h(125)$ mass and production rate measurements at ATLAS and CMS. For the M_h^{125} , $M_h^{125}(\text{alignment})$, $M_h^{125}(\tilde{\chi})$, and $M_h^{125}(\tilde{\tau})$ benchmark scenarios, a significant portion of the parameter space is consistent with the $h(125)$ measurements and with limits from searches for supersymmetry particles and additional Higgs bosons at ATLAS and CMS using pp collisions at $\sqrt{s} = 7, 8$, and 13 TeV [85]. The assumption of a SM width is a reasonable approximation for the MSSM scenarios considered, with relatively small widths predicted with respect to the experimental resolution for the majority of the phase space explored.

Model predictions for the MSSM scenarios are provided by the LHC Higgs Cross Section Working Group [42]. The ggF cross sections have been computed with SUSHi [86, 87], which includes NLO QCD corrections [88], NNLO QCD corrections for the top quark contribution in the effective theory of a heavy top quark [89–91] and electroweak effects by light quarks [92, 93]. For most of the scenarios considered, NLO supersymmetric-QCD corrections [94–97] in expansions of heavy SUSY masses are also included in SUSHi. The masses, mixing angles, and the effective Yukawa couplings of the Higgs bosons for all scenarios except the hMSSM are calculated with FEYNHIGGS [98–104]. The branching fractions for the hMSSM scenario are obtained with HDECAY [105–107], while for all other scenarios the branching fractions are obtained from a combination of FEYNHIGGS, HDECAY

and PROPHECY4F [108, 109]. The results for the general 2HDM interpretation are obtained using the ggF cross sections computed with SUSHi and the branching fractions with 2HDMC [110]. These calculations are compatible with the results from HIGLU [111] and HDECAY within the uncertainties [112]. The VBF cross sections are approximated using the SM Higgs boson production cross sections for VBF, which are provided for different masses by the LHC Higgs Cross Section Working Group [42], multiplied by $\cos^2(\beta - \alpha)$.

6 Selection and categorization

At $\sqrt{s} = 13$ TeV, the ggF cross section for the h(125) is almost one order of magnitude larger than that for VBF production [42]. However, the ggF cross section decreases with m_X while the VBF/ggF cross section ratio increases, meaning that the VBF production mechanism becomes more important at higher masses. The main feature distinguishing the two production mechanisms is the presence of associated forward jets for VBF production. A categorization of events based on both the kinematic properties of associated jets and matrix element techniques is employed to optimize the signal sensitivity. Events with a VBF topology are selected by requiring the presence of two associated jets with an invariant mass of at least 500 GeV and a $\Delta\eta$ greater than 3.5.

6.1 $X \rightarrow 2\ell 2\nu$

The $2\ell 2\nu$ analysis selects two oppositely charged leptons in the same- and different-flavour final states. To suppress the background from nonprompt leptons arising from W+jets production, both leptons must be well identified and isolated. Events are categorized according to the lepton flavour composition and the number of AK4 jets with $p_T > 30$ GeV. To suppress the top quark background, events are required to have no b-tagged AK4 jets with $p_T > 20$ GeV. The final discriminating variable is the reconstructable mass $m_{\text{reco}} = \sqrt{(p_{\ell\ell} + p_T^{\text{miss}})^2 - (\vec{p}_{\ell\ell} + \vec{p}_T^{\text{miss}})^2}$, where $(p_{\ell\ell}, \vec{p}_{\ell\ell})$ is the dilepton four-momentum. This variable is chosen for its effectiveness in discriminating between signal and background, and between different signal mass hypotheses.

6.1.1 Different-flavour final state

For the different-flavour $e\mu$ channel, one of the two leptons is required to have $p_T > 25$ GeV and the other is required to have $p_T > 20$ GeV. To suppress background processes with three or more leptons in the final state, such as ZZ, WZ, or triboson production, events with an additional identified and isolated lepton with $p_T > 10$ GeV are rejected. The dilepton invariant mass $m_{\ell\ell}$ is required to be higher than 50 GeV to reduce the h(125) contamination. Due to the presence of neutrinos in the final state of interest, only events with $p_T^{\text{miss}} > 20$ GeV are considered. The $DY \rightarrow \tau^+\tau^-$ background is suppressed by requiring that the dilepton transverse momentum $p_T^{\ell\ell}$ is above 30 GeV and the X transverse mass $m_T^{\ell\ell}$ is above 60 GeV, where $m_T^{\ell\ell} = \sqrt{2p_T^{\ell\ell}p_T^{\text{miss}}(1 - \cos\Delta\phi^{\ell\ell})}$ and $\Delta\phi^{\ell\ell}$ is the azimuthal angle between \vec{p}_T^{miss} and $\vec{p}_T^{\ell\ell}$. Finally, motivated by the high-mass of the signals under investigation, the condition $m_{\text{reco}} > 100$ GeV must be satisfied.

In this channel four exclusive jet categories are defined: a zero-jet, one-jet, two-jet and VBF category. The last category requires the presence of exactly two jets which satisfy the VBF selection criteria. Dijet events failing these criteria enter the two-jet category. Figure 2 displays the m_{reco} distributions for events passing the $2\ell 2\nu$ different-flavour selection in the four exclusive jet categories.

6.1.2 Same-flavour final state

For the same-flavour e^+e^- and $\mu^+\mu^-$ channels, both leptons are required to have $p_T > 20$ GeV. Events with an additional identified and isolated lepton with $p_T > 10$ GeV are rejected. The background rejection requirements described for the $e\mu$ channel are also applied in these channels. To suppress the large $DY \rightarrow e^+e^-$ and $DY \rightarrow \mu^+\mu^-$ backgrounds only those events with two jets satisfying the VBF selection criteria are considered. For the further reduction of this background, the $m_{\ell\ell}$ and p_T^{miss} requirements are raised to 120 and 50 GeV, respectively. Figure 2 displays the m_{reco} distributions for events passing the $2\ell 2\nu$ same-flavour selection.

6.2 $X \rightarrow \ell\nu 2q$

In the $\ell\nu 2q$ analysis, the $W \rightarrow \ell\nu$ candidates are reconstructed by combining the p_T^{miss} and a lepton which has $p_T > 30$ GeV and $|\eta| < 2.1$ (2.4) for electrons (muons). Those events containing additional electrons (muons) with $p_T > 15$ (10) GeV passing loose identification requirements are rejected. The p_T^{miss} is considered as an estimate of the neutrino p_T with the longitudinal component p_z of the neutrino momentum estimated by imposing a W boson mass constraint to the $\ell\nu$ system and solving the corresponding quadratic equation. The solution with the smallest magnitude of neutrino p_z is chosen. When a real solution is not found, only the real part is considered. The $W \rightarrow q\bar{q}'$ candidates are reconstructed as either high- p_T merged jets or as resolved low- p_T jet pairs. A W boson mass window selection is applied to suppress the W+jets background. If an additional AK4 jet with $p_T > 20$ GeV which is b-tagged is present, then the event is rejected to suppress the top quark background. The $W \rightarrow \ell\nu$ and $W \rightarrow q\bar{q}'$ decay candidates are combined into WW resonance candidates. The final discriminating variable is the invariant mass of the WW system, m_{WW} .

Events are categorized based on the tagging of VBF and ggF production mechanisms. A VBF category is defined by requiring two additional AK4 jets satisfying the VBF selection criteria. Those events failing the VBF selection are considered for the ggF category. The tagging of ggF candidates is achieved using a kinematic discriminant based on the angular distributions of the X candidate decay products. This is implemented with MELA which uses JHUGEN and MCFM matrix elements to calculate probabilities for an event to come from either signal or background, respectively. A WW resonance candidate is considered ggF-tagged if the kinematic discriminant is greater than 0.5. Those events with WW resonance candidates failing this requirement enter the untagged category, resulting in three production mechanism categories.

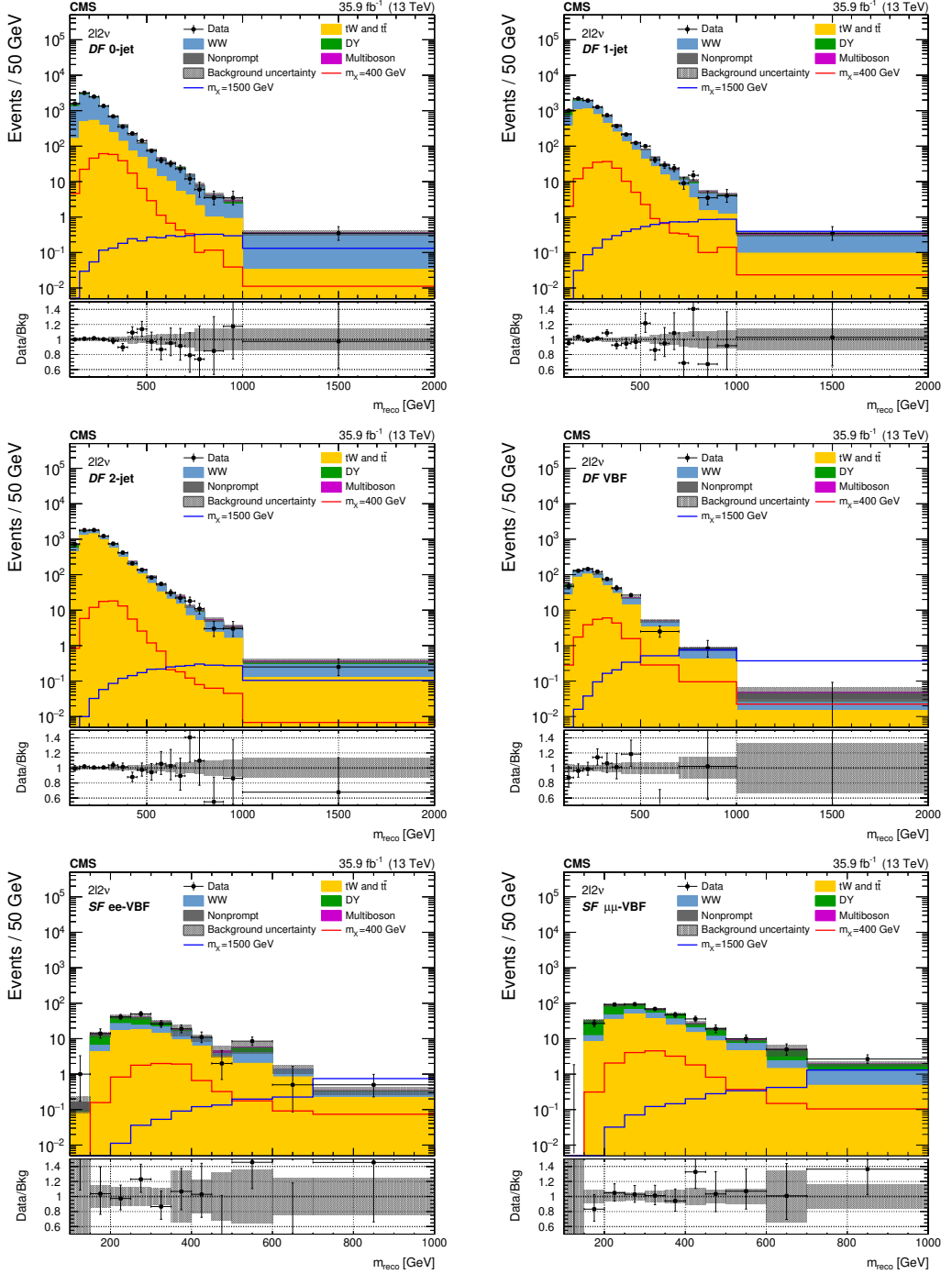


Figure 2. The m_{reco} distributions in the $2\ell 2\nu$ different- (upper and middle) and same-flavour (lower) categories, after performing a background-only fit with the dominant background normalizations determined using control regions. The points represent the data and the stacked histograms the expected backgrounds. Also shown are the sum of the expected ggF- and VBF-produced signals for $m_\chi = 400$ and 1500 GeV, normalized to the SM cross sections, and without considering interference effects. The hatched area shows the combined statistical and systematic uncertainties in the background estimation. Lower panels show the ratio of data to expected background. Larger bin widths are used at higher m_{reco} ; the bin widths are indicated by the horizontal error bars.

6.2.1 Boosted final state

For the boosted final state, an AK8 jet with m_J in the mass window $65 < m_J < 105$ GeV is required. To suppress the background from nonprompt leptons in QCD multijet events, only events with $p_T^{\text{miss}} > 40$ GeV are considered. For heavy-resonance decays the p_T of the W candidates are expected to be roughly half of the resonance mass. Therefore both the leptonic and hadronic W candidates must satisfy the condition $p_T^W/m_{WW} > 0.4$. Finally, to identify boosted W candidates (boosted W tagging) the N -subjettiness ratio τ_{21} is required to be < 0.4 . The m_{WW} distributions for events passing the $\ell\nu 2q$ boosted selection in the three production categories are shown in figure 3.

6.2.2 Resolved final state

For events that do not contain a boosted W-tagged jet with $m_J > 40$ GeV, a resolved hadronic W boson decay reconstruction is attempted using two AK4 jets with $p_T > 30$ GeV and $|\eta| < 2.4$. In events with greater than two jets the selection of the dijet pair is performed by means of a kinematic fit [113]. For each dijet pair the kinematic fit algorithm constrains the jet four-momenta, assuming the dijet invariant mass is that of the W boson, and assigns a χ^2 according to the goodness of the fit. The dijet pair with the smallest χ^2 is chosen as the hadronic W candidate. The invariant mass of the dijet system must be in the mass window $65 < m_{jj} < 105$ GeV. To suppress the background from nonprompt leptons in QCD multijet events, it is required that $p_T^{\text{miss}} > 30$ GeV and that the leptonic W candidate transverse mass m_T^ℓ is above 50 GeV, where $m_T^\ell = \sqrt{2p_T^\ell p_T^{\text{miss}}(1 - \cos \Delta\phi^\ell)}$ and $\Delta\phi^\ell$ is the azimuthal angle between \vec{p}_T^{miss} and the lepton transverse momentum \vec{p}_T^ℓ . The leptonic and hadronic W candidates must also satisfy the condition $p_T^W/m_{WW} > 0.35$. Further reduction in the QCD multijet background is achieved by requiring that the X transverse mass $m_T^{\ell jj}$ is above 60 GeV, where $m_T^{\ell jj} = \sqrt{2p_T^{\ell jj} p_T^{\text{miss}}(1 - \cos \Delta\phi^{\ell jj})}$ and $\Delta\phi^{\ell jj}$ is the azimuthal angle between \vec{p}_T^{miss} and the transverse momentum of the lepton plus jets system $\vec{p}_T^{\ell jj}$. The m_{WW} distributions for events passing the $\ell\nu 2q$ resolved selection in the three production categories are shown in figure 3.

7 Background estimation

The dominant backgrounds are modeled via simulation that has been reweighted to account for known discrepancies between data and simulated events. Corrections associated with the description in simulation of the trigger efficiencies, as well as the efficiency for electron and muon reconstruction, identification, and isolation, are extracted from events with leptonic Z boson decays using a “tag-and-probe” technique [114]. The b tagging efficiency is measured using data samples enriched in b quark jets and corrections for simulation derived [115]. For the $\ell\nu 2q$ boosted category, corrections are applied to the W tagging efficiency and the m_J scale and resolution of W-tagged jets. These corrections have been measured in an almost pure sample of semileptonic $t\bar{t}$ events, where boosted W bosons produced in the top quark decays are separated from the combinatorial $t\bar{t}$ background by means of a simultaneous fit to m_J [116]. For the normalization of the major backgrounds data driven estimates using control regions are employed.

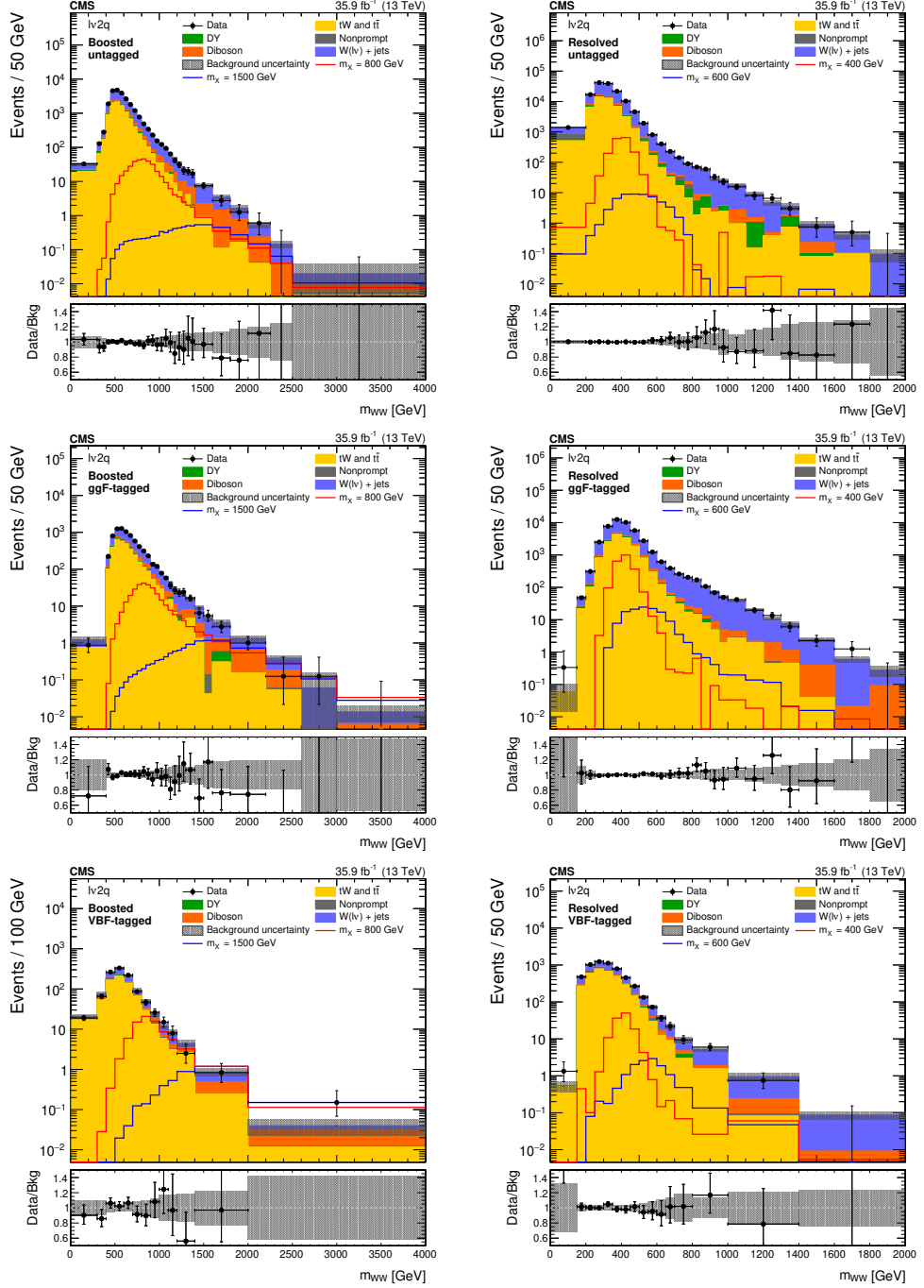


Figure 3. The m_{WW} distributions in the $\ell\nu 2q$ boosted (left) and resolved (right) categories, after performing a background-only fit with the dominant background normalizations determined using control regions. Electron and muon channels are combined. The points represent the data and the stacked histograms the expected backgrounds. Also shown are the sum of the expected ggF- and VBF-produced signals for $m_X = 800$ and 1500 GeV (left), and $m_X = 400$ and 600 GeV (right), normalized to the SM cross sections, and without considering interference effects. The hatched area shows the combined statistical and systematic uncertainties in the background estimation. Lower panels show the ratio of data to expected background. Larger bin widths are used at higher m_{WW} ; the bin widths are indicated by the horizontal error bars.

7.1 $X \rightarrow 2\ell 2\nu$

The main background processes contributing to the $2\ell 2\nu$ final state are from nonresonant WW and top quark production. The nonresonant WW background populates the entire phase space in m_{reco} while the high-mass signal contribution is concentrated at high values of this variable. Therefore, this background is estimated directly in the final fit to the data by allowing the WW normalization to float freely and independently in each category.

The estimation of the top quark background is performed using a top quark enriched data control region, defined by inverting the b jet veto requirement. It is used to constrain the top quark background normalization which is allowed to float freely in the final fit to the data. The estimation is performed separately for each of the different- and same-flavour categories. The m_{reco} distributions in the top quark control regions of each of the different-flavour categories are shown in figure 4. The expected backgrounds before fitting the data are shown, good agreement between the top quark background predictions and the data is observed.

The DY process is a significant source of background in the same-flavour categories. A subleading source of background in the different-flavour categories comes from $DY \rightarrow \tau^+ \tau^-$, where each τ decays leptonically. In the final fit to the data, the DY normalization is also allowed to float freely and independently in each category, and is constrained using control regions which are defined using modified signal region selections. For the different-flavour channel, a DY control region is defined for each jet category by inverting the signal region $m_T^{\ell\ell}$ selection, requiring $m_T^{\ell\ell} < 60$ GeV. The invariant mass of the two leptons is restricted to the interval between 50 and 80 GeV to reduce contributions from nonprompt leptons and from top quark processes. For the same-flavour channels, the control regions are defined by changing the signal region $m_{\ell\ell}$ selection to require $70 < m_{\ell\ell} < 120$ GeV. Discrepancies are observed between the p_T^{miss} distributions in data and simulation for the same-flavour control regions. A linear p_T^{miss} correction is derived for the simulation by fitting the ratio between data, with minor background subtracted, and the DY prediction. The m_{reco} distributions in the DY control regions of each of the same-flavour categories are shown in figure 4. The expected backgrounds before fitting the data are shown, good agreement between the DY background predictions and the data is observed.

The instrumental background arising from nonprompt leptons in W+jets production is estimated to be between 2 and 8% of the total background. An estimate is done in a control region that uses looser lepton identification criteria with relaxed isolation requirements. The probability for a jet that satisfies the loose lepton requirements to also satisfy the standard selection is determined using dijet events. Similarly, the efficiency for a prompt lepton that satisfies the loose lepton identification requirements to also satisfy the standard selection is determined using DY events. These efficiencies are then used to weight the data events with the probability for the event to contain a nonprompt lepton and the relative probability for the candidates in this event to also satisfy the standard selection. Other subleading backgrounds, such as WZ, ZZ, and triboson production, are estimated from simulation.

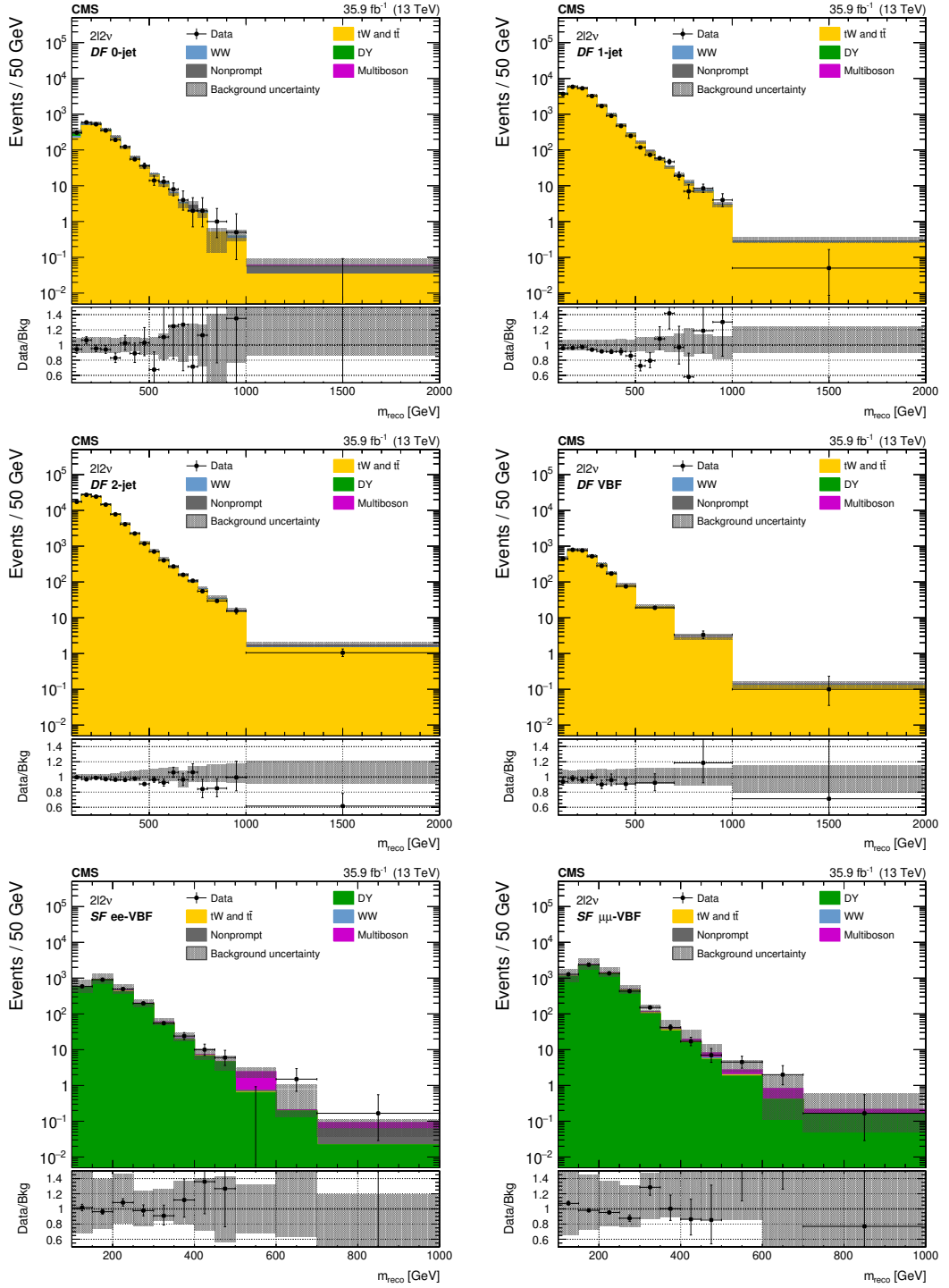


Figure 4. The m_{reco} distributions in the top quark control regions of the $2\ell 2\nu$ different-flavour categories (upper and middle) and the DY control regions of the $2\ell 2\nu$ same-flavour categories (lower). The points represent the data and the stacked histograms show the expected backgrounds. The hatched area shows the combined statistical and systematic uncertainties in the background estimation. Lower panels show the ratio of data to expected background. Larger bin widths are used at higher m_{reco} ; the bin widths are indicated by the horizontal error bars.

7.2 $X \rightarrow 2\nu 2q$

The main backgrounds for the $\ell\nu 2q$ analysis are from W+jets and top quark production, with subdominant contributions from diboson, DY, and QCD multijet production.

The majority of the events passing the $\ell\nu 2q$ selection come from W+jets and top quark production. An estimate of the W+jets and top quark background normalizations using two control regions in data is employed. A top quark enriched data control region is defined reversing the b jet veto, by requiring events with an additional jet which is b-tagged. Additionally, a sideband control region, with a similar background composition to that of the signal region, is defined by adapting the hadronic W candidate mass requirements of the signal region selection. In the boosted (resolved) category m_J (m_{jj}) is required to be outside the W boson mass window (65–105 GeV) and within the range $40 < m_J$ (m_{jj}) < 250 GeV. In the final fit to the data, the normalizations of both the W+jets and top quark backgrounds are allowed to float freely, with the observed yields in the control regions used to constrain the normalizations. This background estimation procedure is applied independently in each category.

The contamination from diboson events represents 6 and 3% of the total background in the boosted and resolved categories, respectively. Production of WW, WZ, and ZZ through $q\bar{q}$ annihilation is estimated directly from simulation while the $gg \rightarrow WW$ and $qq \rightarrow qqWW$ backgrounds are estimated through the reweighting of signal samples using MELA.

The DY contamination is suppressed due to the second-lepton veto. It is estimated directly from simulation and represents between 1 and 2% of the total background.

Contamination from nonprompt leptons in QCD multijet production is estimated from simulation to be between 1 and 2% of the total background. The contribution from this source is largely suppressed due to the W candidate p_T , transverse mass, and substructure requirements. The QCD multijet enriched samples are defined through a reversal of these requirements, allowing a test of the multijet simulation. The resolved selection is altered by requiring $m_T^\ell < 50$ GeV, $m_T^{\ell jj} < 60$ GeV, and $p_T^W/m_{WW} < 0.35$, while for the boosted selection it is required that $m_T^\ell < 50$ GeV, $\tau_{21} > 0.4$, and $p_T^W/m_{WW} < 0.4$. The QCD multijet contamination levels attained are 35 and 14% in the boosted and resolved categories, respectively. After subtracting the estimated prompt-lepton backgrounds, the predicted number of QCD multijet events in each category is found to agree with the data within 3%, with the statistical uncertainties of the order of 10%.

To help verify the background estimation procedure, a fit is performed to the m_{WW} distributions in the sideband allowing the W+jets and top quark background normalizations to float freely. The observed yield in the top quark control region is included in the fit to help constrain the top quark background normalization. Figure 5 shows the result of the fit to the sideband m_{WW} distributions for the boosted and resolved categories. A good level of agreement between data and the background predictions is observed.

8 Signal extraction and systematic uncertainties

The methodology used to interpret the data and to combine the results from independent categories has been developed by the ATLAS and CMS collaborations in the context of

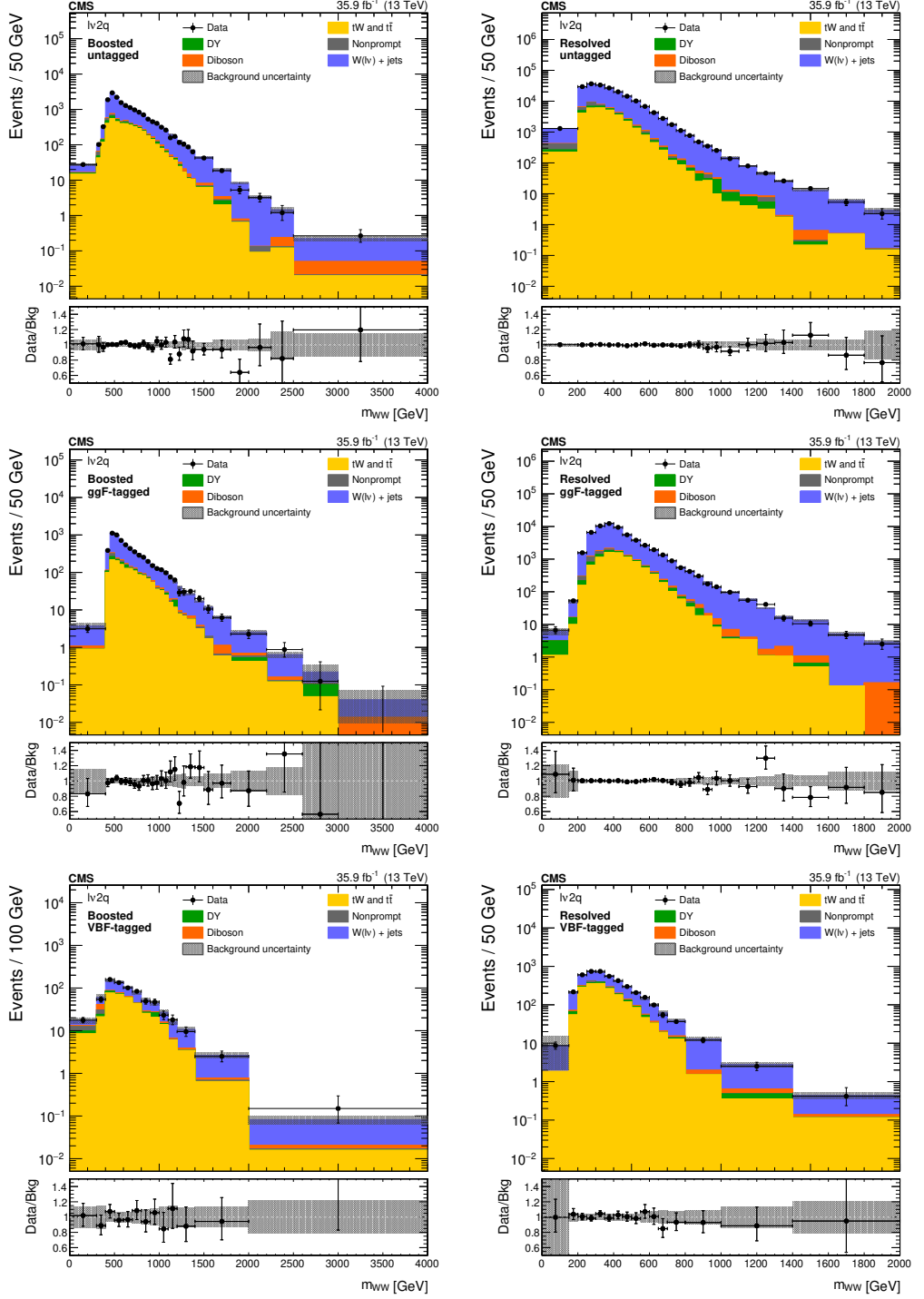


Figure 5. The m_{WW} distributions in the sideband control regions of the $\ell\nu 2q$ boosted (left) and resolved (right) categories, after fitting the sideband data with the top quark background normalization determined using a control region. Electron and muon channels are combined. The points represent the data and the stacked histograms show the expected backgrounds. The hatched area shows the combined statistical and systematic uncertainties in the background estimation. Lower panels show the ratio of data to expected background. Larger bin widths are used at higher m_{WW} ; the bin widths are indicated by the horizontal error bars.

the LHC Higgs Combination Group. A general description of the method can be found in refs. [117–119].

The signal extraction procedure is based on a combined binned maximum likelihood fit of the discriminant distributions with signal and background templates, performed simultaneously in all the $\ell\nu 2q$ and $2\ell 2\nu$ signal region categories. Signal templates for both the ggF and VBF production modes are included in the fit, with a number of hypotheses for f_{VBF} considered. The various control regions used to constrain the dominant backgrounds are included in the form of single bins, representing the number of events in each control region. The dominant background normalizations are initially unconstrained and are determined during the fit. After fitting the data the uncertainties on the WW, top quark and DY background normalizations in the $2\ell 2\nu$ categories are in the range 6–45%, 3–5%, and 5–20%, respectively. In the $\ell\nu 2q$ categories, the corresponding uncertainties on the W+jets and top quark background normalizations are in the range 7–10% and 4–20%, respectively. The remaining systematic uncertainties are represented by individual nuisance parameters with a log-normal model used for normalization uncertainties and a Gaussian model used for shape uncertainties. For each source of uncertainty, the correlations between different categories, and different signal and background processes, are taken into account. Uncertainties arising from limited number of events in the MC simulated samples are included for each bin of the discriminant distributions, in each category independently, following the Barlow-Beeston approach [120]. Depending on the category, the statistical uncertainties due to the MC simulated sample sizes on the background and signal normalisations are in the range 1–8%.

The theoretical sources of uncertainty considered include the effect of PDFs and the strong coupling constant α_S , and the effect of missing higher-order corrections via variations of the renormalization and factorization scales. Acceptance uncertainties are evaluated for signal and background by varying the PDFs and α_S within their uncertainties [121], and by varying the factorization and renormalization scales up and down by a factor of two [122]. Depending on the process and the category, the PDF uncertainties in the signal and background yields amount to 1–7%, while those of the renormalization and factorization scales are within 1–18%. The PDF, and the renormalization and factorization scales uncertainties in the signal cross section, computed by the LHC Higgs Cross Section Working Group [42], are also considered and amount to 2–16% and 0.2–9%, respectively, depending on the resonance mass and production mechanism.

Effects due to experimental uncertainties are studied by applying a scaling and/or smearing of certain variables of the physics objects in the simulation, followed by a subsequent recalculation of all the correlated variables. The uncertainty in the measured luminosity is 2.5% for data collected during 2016 [123]. The trigger efficiency uncertainties are approximately 1 and 2% for the $\ell\nu 2q$ and $2\ell 2\nu$ final states, respectively. Lepton reconstruction and identification efficiency uncertainties vary between 1 and 3%, while the muon momentum and electron energy scale uncertainties amount to 0.1–1.0% each. Depending on the process and the category, the jet energy scale uncertainties are in the range 1–10%. The p_T^{miss} uncertainty is taken into account by propagating the corresponding uncertainties in the leptons and jets and amounts to 0.1–1%. The scale factors correcting the b tagging

efficiency and mistag rate are varied within their uncertainties with resulting uncertainties of 0.1–5% depending on the process and the category. This systematic uncertainty affects the top quark control regions and the signal regions in an anticorrelated way.

In addition, for each final state there are channel-specific uncertainties which are now discussed.

8.1 $X \rightarrow 2\ell 2\nu$

A conservative 30% uncertainty in the normalization of the instrumental background arising from nonprompt leptons in W +jets production is estimated by varying the jet p_T threshold in the dijet control sample used in the background prediction procedure, and from propagation of the statistical uncertainties in the measured lepton misidentification probabilities. Uncertainties of 3–10% due to the p_T^{WW} reweighting are evaluated by varying the factorization and renormalization scales up and down by a factor of two, and by varying the resummation scale. The UE uncertainty for the WW background is estimated by comparing two different UE tunes, while the PS modeling uncertainty is estimated by comparing samples interfaced with different PS models, as described in section 3. The combined effect is evaluated to be 5–10%. A dedicated nuisance parameter for the linear p_T^{miss} correction in the same-flavour DY control region is introduced. The uncertainty is 0.2–1%, estimated with the maximum and minimum best fit lines of the linear fit used to derive the correction. The categorization of events based on jet multiplicity introduces additional signal uncertainties related to higher-order corrections. These uncertainties are associated with the ggF production mode and are evaluated independently following the method described in ref. [124] and are about 5% for the 0-jet, 10% for the 1-jet, and 20% for the 2-jet and VBF categories.

8.2 $X \rightarrow \ell\nu 2q$

The diboson and DY production cross sections are each assigned an uncertainty of 10% based on the level of agreement between theoretical predictions and cross section measurements at CMS using 13 TeV data [125, 126]. An uncertainty of 10% in the normalization of the background arising from nonprompt leptons in QCD multijet production is assigned based on the observed level of agreement between data and simulation in QCD multijet enriched samples. The impact of the jet energy resolution uncertainty is about 0.3–2%, depending on the process and the category. For W -tagged jets the m_J scale and resolution uncertainties are evaluated to be 0.1–1 and 2–5%, respectively. The τ_{21} scale factor correcting the boosted W tagging efficiency has an associated uncertainty of 6%. Since this is measured in $t\bar{t}$ events using jets with a typical p_T of 200 GeV, an uncertainty of 1–13% in the extrapolation to the higher- p_T regime of the high-mass signal is also included.

A summary of the systematic uncertainties included for the $\ell\nu 2q$ and $2\ell 2\nu$ final states are shown in table 1.

9 Results

No evidence for an excess of events with respect to the SM predictions is observed. Upper exclusion limits at 95% confidence level (CL) on the X cross section times branching fraction

Source of uncertainty	$X \rightarrow WW \rightarrow 2\ell 2\nu$	$X \rightarrow WW \rightarrow \ell\nu 2q$	$X \rightarrow WW \rightarrow \ell\nu 2q$
		Resolved	Boosted
Experimental sources			
Integrated luminosity	2.5%	2.5%	2.5%
Lepton trigger*	2%	1%	1%
Lepton reconstruction & ident.*	1–3%	1–2%	1–2%
Electron energy scale*	0.1–1%	0.2–1%	0.1–1%
Muon momentum scale*	0.1–1%	0.1–1%	0.1–1%
Jet energy scale*	1–10%	1–6%	1–3%
Jet energy resolution*	—	0.5–2%	0.3–1%
$p_{\text{T}}^{\text{miss}}$ *	0.1–1%	1–3%	0.1–1%
b tagging/mistag*	0.1–5%	0.1–1%	0.1–1%
W tagging (τ_{21})	—	—	6%
W tagging (extrapolation)	—	—	1–13%
W m_{J} scale	—	—	0.1–1%
W m_{J} resolution	—	—	2–5%
Background estimates			
WW	6–45%	10%	10%
top quark	3–5%	7–9%	8–10%
W+jets	30%	5–11%	4–20%
QCD multijet	—	10%	10%
DY	5–20%	10%	10%
Theoretical sources			
PDF and α_{S} (acceptance)*	1–4%	1–4%	1–7%
Renorm./factor. scales (acceptance)*	1–6%	1–18%	1–18%
PDF and α_{S} (σ_{X})	2–16%	2–4%	2–16%
Renorm./factor. scales (σ_{X})	0.2–9%	0.2–4%	0.2–9%
Jet multiplicity categorization ($\sigma_{\text{gg} \rightarrow \text{X}}$)*	5–20%	—	—
WW p_{T}^{WW} reweighting*	3–10%	—	—
WW UE & PS	5–10%	—	—
DY $p_{\text{T}}^{\text{miss}}$ reweighting*	0.2–1%	—	—
Other sources			
MC statistics*	1–5%	1–8%	1–5%

Table 1. Summary of systematic uncertainties, quoted in percent, affecting the normalization of the background and signal samples. The uncertainties on the WW, top quark and DY (W+jets and top quark) background estimates in the $2\ell 2\nu$ ($\ell\nu 2q$) categories have been determined during the fit to the data. The numbers shown as ranges represent the uncertainties for different processes and categories. Missing values represent uncertainties either estimated to be negligible ($<0.1\%$), or not applicable in a specific channel. Those systematic uncertainties found to affect the shape of kinematic distributions are labeled with *.

of the decay to two W bosons are evaluated for masses between 0.2 and 3.0 TeV using the asymptotic modified frequentist method (CL_s) [117–119]. A number of hypotheses for f_{VBF} have been investigated by setting this fraction to the SM value, by allowing it to float, and by setting $f_{\text{VBF}} = 0$ and 1. The expected and observed exclusion limits for the full combination of the $2\ell 2\nu$ and $\ell\nu 2q$ analyses are shown in figure 6. For signals below ≈ 800 GeV, the sensitivity of the $2\ell 2\nu$ final state is dominated by the different-flavour channel, while at higher masses the same- and different-flavour channels have similar sensitivities. For the $\ell\nu 2q$ final state, the sensitivity is dominated by the boosted channel for

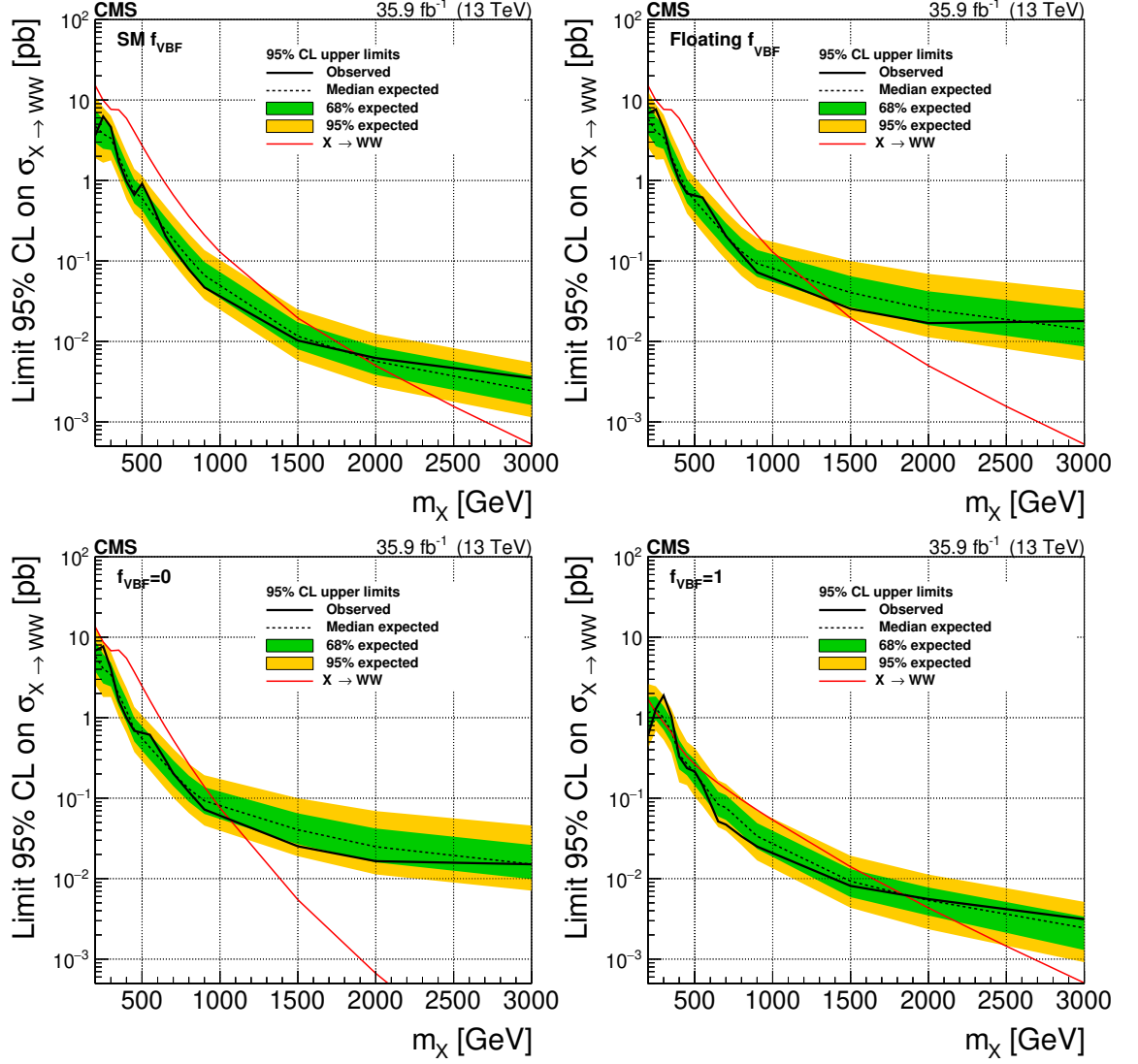


Figure 6. Expected and observed exclusion limits at 95% CL on the X cross section times branching fraction to WW for a number of f_{VBF} hypotheses. For the SM f_{VBF} (upper left) and floating f_{VBF} (upper right) cases the red line represents the sum of the SM cross sections for ggF and VBF production, while for the $f_{\text{VBF}} = 0$ (lower left) and the $f_{\text{VBF}} = 1$ (lower right) cases it represents the ggF and VBF production cross sections, respectively. The black dotted line corresponds to the central expected value while the yellow and green bands represent the 68 and 95% CL uncertainties, respectively.

signals above ≈ 400 GeV, while at lower masses the resolved channel dominates. Comparing the two final states, the $2\ell 2\nu$ sensitivity is dominant up to ≈ 400 GeV, while at higher masses the $\ell\nu 2q$ final state is more sensitive by a factor of approximately two. Comparing the excluded cross section values to the expectations from theoretical calculations, a X signal is excluded up to 1870 (1370) GeV with f_{VBF} set to the SM value (f_{VBF} allowed to float). A X signal is excluded up to 1060 GeV for the $f_{\text{VBF}} = 0$ hypothesis, while the mass ranges 200–245 and 380–1840 GeV are excluded for the $f_{\text{VBF}} = 1$ hypothesis.

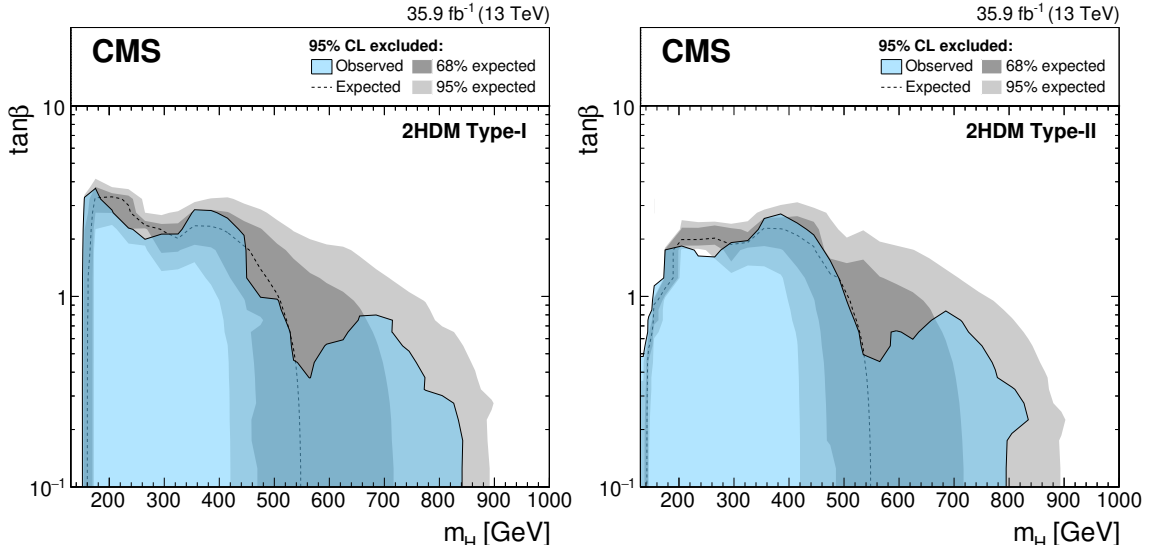


Figure 7. Expected and observed 95% CL upper limits on $\tan\beta$ as a function of m_H for a Type-I (left) and Type-II (right) 2HDMs. It is assumed that $m_H = m_A = m_{H^\pm}$ and $\cos(\beta - \alpha) = 0.1$. The expected limit is shown as a dashed black line while the dark and light gray bands indicate the 68 and 95% CL uncertainties, respectively. The observed exclusion contour is indicated by the blue area.

Exclusion limits are also set for neutral heavy Higgs bosons in the context of a Type-I and Type-II 2HDM, with the assumptions that $m_H = m_A = m_{H^\pm}$ and $\cos(\beta - \alpha) = 0.1$. Figure 7 shows the expected and observed exclusion limits in the m_H - $\tan\beta$ plane. The dashed lines mark the expected limits while the dark and bright gray bands indicate the 68 and 95% CL uncertainties, respectively. The observed exclusion contours are indicated by the blue areas. In both scenarios, the observed exclusion contours reach m_H values of ≈ 800 GeV, while the maximum $\tan\beta$ value excluded is ≈ 3 . Figure 8 shows the expected and observed exclusion limits for the $m_h^{\text{mod}+}$ and the hMSSM scenarios. The maximum $\tan\beta$ value excluded for both scenarios is ≈ 9 , while the maximum value of m_A excluded is ≈ 430 GeV. The exclusion of the regions at low values of m_A and $\tan\beta$ complement the exclusion limits set by the MSSM $H \rightarrow \tau^+\tau^-$ analyses from ATLAS and CMS using 13 TeV data [127, 128], which have reduced sensitivity in these regions. Figure 9 shows the expected and observed exclusion limits for the M_h^{125} , $M_h^{125}(\text{alignment})$, $M_h^{125}(\tilde{\chi})$, and $M_h^{125}(\tilde{\tau})$ scenarios. Low values of m_A and $\tan\beta$ are also excluded for these scenarios. The observed exclusion contours reach m_A values of ≈ 400 GeV, while the maximum $\tan\beta$ values excluded are in the range 5–9. These results further reduce the allowed parameter space for extensions of the SM.

10 Summary

A search for a heavy Higgs boson decaying to a pair of W bosons in the mass range from 0.2 to 3.0 TeV has been presented. The data analysed were collected by the CMS experiment at the LHC in 2016, corresponding to an integrated luminosity of 35.9 fb^{-1} at $\sqrt{s} = 13 \text{ TeV}$.

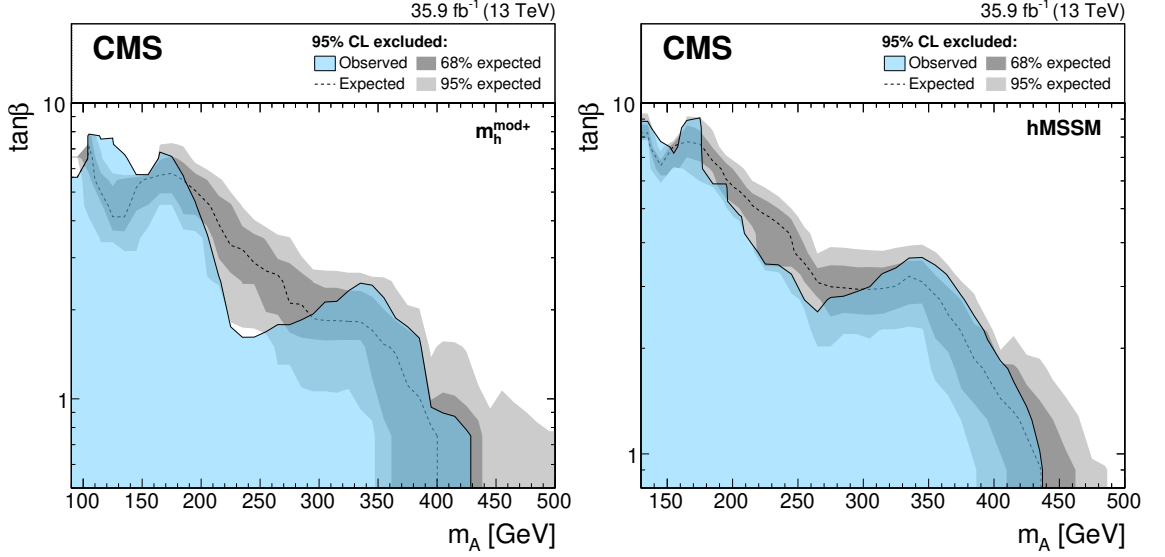


Figure 8. Expected and observed 95% CL upper limits on $\tan \beta$ as a function of m_A for the $m_h^{\text{mod}+}$ (left) and hMSSM (right) scenarios. The expected limit is shown as a dashed black line while the dark and light gray bands indicate the 68 and 95% CL uncertainties, respectively. The observed exclusion contour is indicated by the blue area.

The W boson pair decays are reconstructed in the $2\ell 2\nu$ and $\ell\nu 2q$ final states. Both gluon fusion and vector boson fusion production of the signal are considered, with a number of hypotheses for their relative contributions investigated. Interference effects between the signal and background are also taken into account. Dedicated event categorizations based on both the kinematic properties of associated jets and matrix element techniques are employed to optimize the signal sensitivity. No evidence for an excess of events with respect to the standard model (SM) predictions is observed. Combined upper limits at 95% confidence level on the product of the cross section and branching fraction exclude a heavy Higgs boson with SM-like couplings and decays up to 1870 GeV. Exclusion limits are also set in the context of a number of two-Higgs-doublet model formulations, further reducing the allowed parameter space for extensions of the SM.

Acknowledgments

We congratulate our colleagues in the CERN accelerator departments for the excellent performance of the LHC and thank the technical and administrative staffs at CERN and at other CMS institutes for their contributions to the success of the CMS effort. In addition, we gratefully acknowledge the computing centres and personnel of the Worldwide LHC Computing Grid for delivering so effectively the computing infrastructure essential to our analyses. Finally, we acknowledge the enduring support for the construction and operation of the LHC and the CMS detector provided by the following funding agencies: BMBWF and FWF (Austria); FNRS and FWO (Belgium); CNPq, CAPES, FAPERJ, FAPERGS, and FAPESP (Brazil); MES (Bulgaria); CERN; CAS, MoST, and NSFC (China); COL-

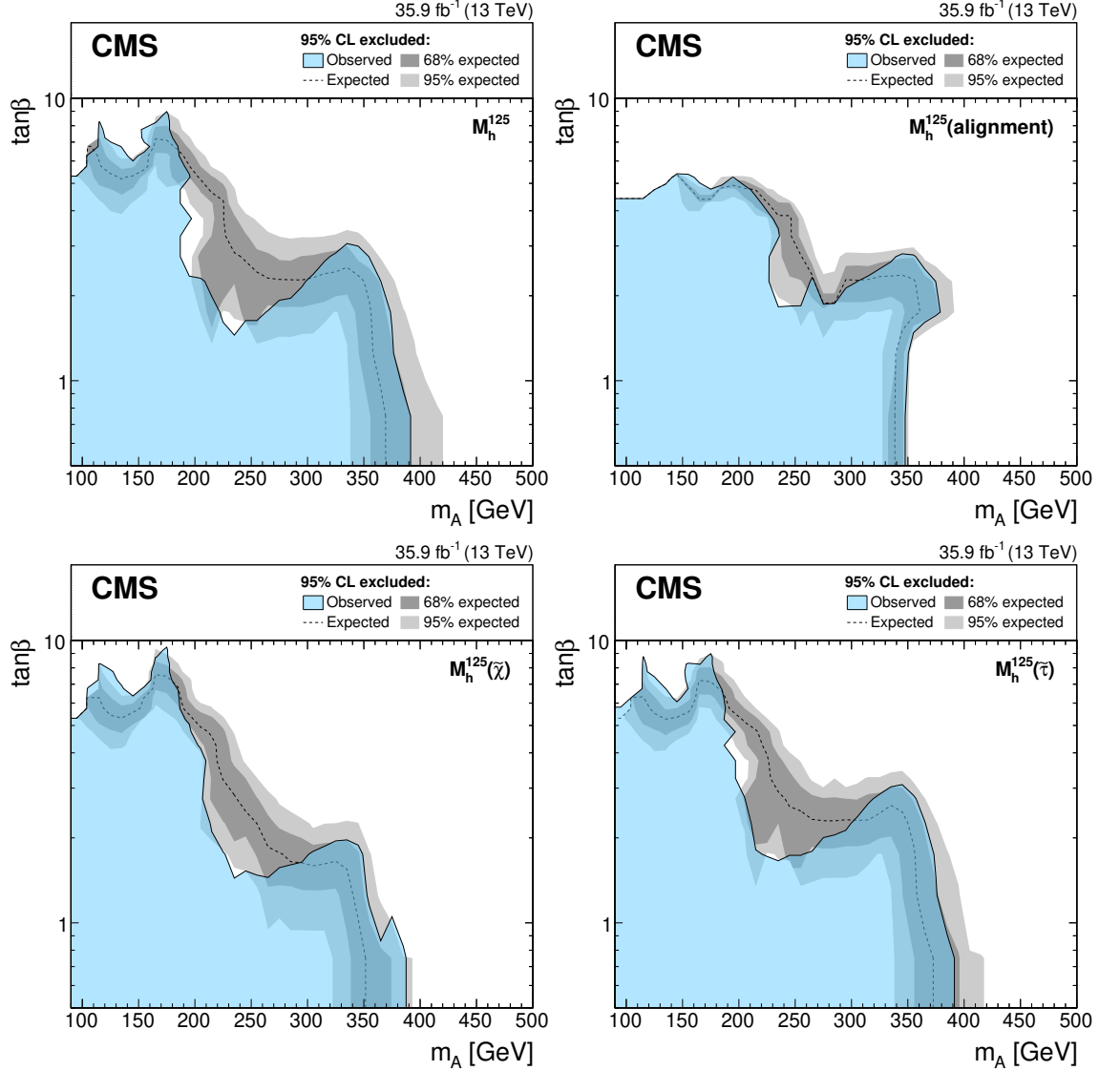


Figure 9. Expected and observed 95% CL upper limits on $\tan\beta$ as a function of m_A for the M_h^{125} (upper left), $M_h^{125}(\text{alignment})$ (upper right), $M_h^{125}(\tilde{\chi})$ (lower left), and $M_h^{125}(\tilde{\tau})$ (lower right) scenarios. The expected limit is shown as a dashed black line while the dark and light gray bands indicate the 68 and 95% CL uncertainties, respectively. The observed exclusion contour is indicated by the blue area.

CIENCIAS (Colombia); MSES and CSF (Croatia); RPF (Cyprus); SENESCYT (Ecuador); MoER, ERC IUT, PUT and ERDF (Estonia); Academy of Finland, MEC, and HIP (Finland); CEA and CNRS/IN2P3 (France); BMBF, DFG, and HGF (Germany); GSRT (Greece); NKFI (Hungary); DAE and DST (India); IPM (Iran); SFI (Ireland); INFN (Italy); MSIP and NRF (Republic of Korea); MES (Latvia); LAS (Lithuania); MOE and UM (Malaysia); BUAP, CINVESTAV, CONACYT, LNS, SEP, and UASLP-FAI (Mexico); MOS (Montenegro); MBIE (New Zealand); PAEC (Pakistan); MSHE and NSC (Poland); FCT (Portugal); JINR (Dubna); MON, RosAtom, RAS, RFBR, and NRC KI (Russia);

MESTD (Serbia); SEIDI, CPAN, PCTI, and FEDER (Spain); MOSTR (Sri Lanka); Swiss Funding Agencies (Switzerland); MST (Taipei); ThEPCenter, IPST, STAR, and NSTDA (Thailand); TUBITAK and TAEK (Turkey); NASU (Ukraine); STFC (United Kingdom); DOE and NSF (U.S.A.).

Individuals have received support from the Marie-Curie programme and the European Research Council and Horizon 2020 Grant, contract Nos. 675440, 752730, and 765710 (European Union); the Leventis Foundation; the A.P. Sloan Foundation; the Alexander von Humboldt Foundation; the Belgian Federal Science Policy Office; the Fonds pour la Formation à la Recherche dans l’Industrie et dans l’Agriculture (FRIA-Belgium); the Agentschap voor Innovatie door Wetenschap en Technologie (IWT-Belgium); the F.R.S.-FNRS and FWO (Belgium) under the “Excellence of Science — EOS” — be.h project n. 30820817; the Beijing Municipal Science & Technology Commission, No. Z181100004218003; the Ministry of Education, Youth and Sports (MEYS) of the Czech Republic; the Deutsche Forschungsgemeinschaft (DFG) under Germany’s Excellence Strategy — EXC 2121 “Quantum Universe” — 390833306; the Lendület (“Momentum”) Programme and the János Bolyai Research Scholarship of the Hungarian Academy of Sciences, the New National Excellence Program ÚNKP, the NKFIA research grants 123842, 123959, 124845, 124850, 125105, 128713, 128786, and 129058 (Hungary); the Council of Science and Industrial Research, India; the HOMING PLUS programme of the Foundation for Polish Science, cofinanced from European Union, Regional Development Fund, the Mobility Plus programme of the Ministry of Science and Higher Education, the National Science Center (Poland), contracts Harmonia 2014/14/M/ST2/00428, Opus 2014/13/B/ST2/02543, 2014/15/B/ST2/03998, and 2015/19/B/ST2/02861, Sonata-bis 2012/07/E/ST2/01406; the National Priorities Research Program by Qatar National Research Fund; the Ministry of Science and Education, grant no. 3.2989.2017 (Russia); the Programa Estatal de Fomento de la Investigación Científica y Técnica de Excelencia María de Maeztu, grant MDM-2015-0509 and the Programa Severo Ochoa del Principado de Asturias; the Thalís and Aristeia programmes cofinanced by EU-ESF and the Greek NSRF; the Rachadapisek Sompot Fund for Postdoctoral Fellowship, Chulalongkorn University and the Chulalongkorn Academic into Its 2nd Century Project Advancement Project (Thailand); the Nvidia Corporation; the Welch Foundation, contract C-1845; and the Weston Havens Foundation (U.S.A.).

Open Access. This article is distributed under the terms of the Creative Commons Attribution License ([CC-BY 4.0](https://creativecommons.org/licenses/by/4.0/)), which permits any use, distribution and reproduction in any medium, provided the original author(s) and source are credited.

References

- [1] ATLAS collaboration, *Observation of a new particle in the search for the Standard Model Higgs boson with the ATLAS detector at the LHC*, *Phys. Lett. B* **716** (2012) 1 [[arXiv:1207.7214](https://arxiv.org/abs/1207.7214)] [[INSPIRE](#)].
- [2] CMS collaboration, *Observation of a New Boson at a Mass of 125 GeV with the CMS Experiment at the LHC*, *Phys. Lett. B* **716** (2012) 30 [[arXiv:1207.7235](https://arxiv.org/abs/1207.7235)] [[INSPIRE](#)].

- [3] CMS collaboration, *Observation of a New Boson with Mass Near 125 GeV in pp Collisions at $\sqrt{s} = 7$ and 8 TeV*, *JHEP* **06** (2013) 081 [[arXiv:1303.4571](#)] [[INSPIRE](#)].
- [4] ATLAS collaboration, *Study of the spin and parity of the Higgs boson in diboson decays with the ATLAS detector*, *Eur. Phys. J. C* **75** (2015) 476 [Erratum *ibid.* **C 76** (2016) 152] [[arXiv:1506.05669](#)] [[INSPIRE](#)].
- [5] ATLAS collaboration, *Combined measurements of Higgs boson production and decay using up to 80 fb⁻¹ of proton-proton collision data at $\sqrt{s} = 13$ TeV collected with the ATLAS experiment*, *Phys. Rev. D* **101** (2020) 012002 [[arXiv:1909.02845](#)] [[INSPIRE](#)].
- [6] ATLAS collaboration, *Combined measurement of differential and total cross sections in the $H \rightarrow \gamma\gamma$ and the $H \rightarrow ZZ^* \rightarrow 4\ell$ decay channels at $\sqrt{s} = 13$ TeV with the ATLAS detector*, *Phys. Lett. B* **786** (2018) 114 [[arXiv:1805.10197](#)] [[INSPIRE](#)].
- [7] ATLAS collaboration, *Constraints on off-shell Higgs boson production and the Higgs boson total width in $ZZ \rightarrow 4\ell$ and $ZZ \rightarrow 2\ell 2\nu$ final states with the ATLAS detector*, *Phys. Lett. B* **786** (2018) 223 [[arXiv:1808.01191](#)] [[INSPIRE](#)].
- [8] ATLAS collaboration, *Measurement of the Higgs boson coupling properties in the $H \rightarrow ZZ^* \rightarrow 4\ell$ decay channel at $\sqrt{s} = 13$ TeV with the ATLAS detector*, *JHEP* **03** (2018) 095 [[arXiv:1712.02304](#)] [[INSPIRE](#)].
- [9] ATLAS and CMS collaborations, *Measurements of the Higgs boson production and decay rates and constraints on its couplings from a combined ATLAS and CMS analysis of the LHC pp collision data at $\sqrt{s} = 7$ and 8 TeV*, *JHEP* **08** (2016) 045 [[arXiv:1606.02266](#)] [[INSPIRE](#)].
- [10] CMS collaboration, *Combined search for anomalous pseudoscalar HVV couplings in $VH(H \rightarrow b\bar{b})$ production and $H \rightarrow VV$ decay*, *Phys. Lett. B* **759** (2016) 672 [[arXiv:1602.04305](#)] [[INSPIRE](#)].
- [11] CMS collaboration, *Constraints on anomalous Higgs boson couplings using production and decay information in the four-lepton final state*, *Phys. Lett. B* **775** (2017) 1 [[arXiv:1707.00541](#)] [[INSPIRE](#)].
- [12] CMS collaboration, *Measurements of the Higgs boson width and anomalous HVV couplings from on-shell and off-shell production in the four-lepton final state*, *Phys. Rev. D* **99** (2019) 112003 [[arXiv:1901.00174](#)] [[INSPIRE](#)].
- [13] CMS collaboration, *Measurement and interpretation of differential cross sections for Higgs boson production at $\sqrt{s} = 13$ TeV*, *Phys. Lett. B* **792** (2019) 369 [[arXiv:1812.06504](#)] [[INSPIRE](#)].
- [14] CMS collaboration, *Combined measurements of Higgs boson couplings in proton-proton collisions at $\sqrt{s} = 13$ TeV*, *Eur. Phys. J. C* **79** (2019) 421 [[arXiv:1809.10733](#)] [[INSPIRE](#)].
- [15] CMS collaboration, *Constraints on anomalous HVV couplings from the production of Higgs bosons decaying to τ lepton pairs*, *Phys. Rev. D* **100** (2019) 112002 [[arXiv:1903.06973](#)] [[INSPIRE](#)].
- [16] C. Englert et al., *Precision Measurements of Higgs Couplings: Implications for New Physics Scales*, *J. Phys. G* **41** (2014) 113001 [[arXiv:1403.7191](#)] [[INSPIRE](#)].
- [17] T. Plehn, D.L. Rainwater and D. Zeppenfeld, *Determining the Structure of Higgs Couplings at the LHC*, *Phys. Rev. Lett.* **88** (2002) 051801 [[hep-ph/0105325](#)] [[INSPIRE](#)].

- [18] I. Anderson et al., *Constraining Anomalous HVV Interactions at Proton and Lepton Colliders*, *Phys. Rev. D* **89** (2014) 035007 [[arXiv:1309.4819](#)] [[INSPIRE](#)].
- [19] F. Bishara, U. Haisch, P.F. Monni and E. Re, *Constraining Light-Quark Yukawa Couplings from Higgs Distributions*, *Phys. Rev. Lett.* **118** (2017) 121801 [[arXiv:1606.09253](#)] [[INSPIRE](#)].
- [20] M. Grazzini, A. Ilnicka, M. Spira and M. Wiesemann, *Modeling BSM effects on the Higgs transverse-momentum spectrum in an EFT approach*, *JHEP* **03** (2017) 115 [[arXiv:1612.00283](#)] [[INSPIRE](#)].
- [21] V. Barger, P. Langacker, M. McCaskey, M.J. Ramsey-Musolf and G. Shaughnessy, *LHC Phenomenology of an Extended Standard Model with a Real Scalar Singlet*, *Phys. Rev. D* **77** (2008) 035005 [[arXiv:0706.4311](#)] [[INSPIRE](#)].
- [22] G.C. Branco, P.M. Ferreira, L. Lavoura, M.N. Rebelo, M. Sher and J.P. Silva, *Theory and phenomenology of two-Higgs-doublet models*, *Phys. Rept.* **516** (2012) 1 [[arXiv:1106.0034](#)] [[INSPIRE](#)].
- [23] ATLAS collaboration, *Search for a high-mass Higgs boson decaying to a W boson pair in pp collisions at $\sqrt{s} = 8$ TeV with the ATLAS detector*, *JHEP* **01** (2016) 032 [[arXiv:1509.00389](#)] [[INSPIRE](#)].
- [24] ATLAS collaboration, *Search for an additional, heavy Higgs boson in the $H \rightarrow ZZ$ decay channel at $\sqrt{s} = 8$ TeV in pp collision data with the ATLAS detector*, *Eur. Phys. J. C* **76** (2016) 45 [[arXiv:1507.05930](#)] [[INSPIRE](#)].
- [25] ATLAS collaboration, *Search for heavy resonances decaying into WW in the $e\nu\mu\nu$ final state in pp collisions at $\sqrt{s} = 13$ TeV with the ATLAS detector*, *Eur. Phys. J. C* **78** (2018) 24 [[arXiv:1710.01123](#)] [[INSPIRE](#)].
- [26] ATLAS collaboration, *Search for heavy ZZ resonances in the $\ell^+\ell^-\ell^+\ell^-$ and $\ell^+\ell^-\nu\bar{\nu}$ final states using proton-proton collisions at $\sqrt{s} = 13$ TeV with the ATLAS detector*, *Eur. Phys. J. C* **78** (2018) 293 [[arXiv:1712.06386](#)] [[INSPIRE](#)].
- [27] CMS collaboration, *Search for a Higgs boson in the mass range from 145 to 1000 GeV decaying to a pair of W or Z bosons*, *JHEP* **10** (2015) 144 [[arXiv:1504.00936](#)] [[INSPIRE](#)].
- [28] CMS collaboration, *Search for a new scalar resonance decaying to a pair of Z bosons in proton-proton collisions at $\sqrt{s} = 13$ TeV*, *JHEP* **06** (2018) 127 [Erratum *JHEP* **03** (2019) 128] [[arXiv:1804.01939](#)] [[INSPIRE](#)].
- [29] N. Kauer and C. O'Brien, *Heavy Higgs signal-background interference in $gg \rightarrow VV$ in the Standard Model plus real singlet*, *Eur. Phys. J. C* **75** (2015) 374 [[arXiv:1502.04113](#)] [[INSPIRE](#)].
- [30] S.P. Martin, *A Supersymmetry primer*, *Adv. Ser. Direct. High Energy Phys.* **18** (1998) 1 [[hep-ph/9709356](#)] [[INSPIRE](#)].
- [31] J.E. Kim, *Light Pseudoscalars, Particle Physics and Cosmology*, *Phys. Rept.* **150** (1987) 1 [[INSPIRE](#)].
- [32] J.M. Cline, K. Kainulainen and M. Trott, *Electroweak Baryogenesis in Two Higgs Doublet Models and B meson anomalies*, *JHEP* **11** (2011) 089 [[arXiv:1107.3559](#)] [[INSPIRE](#)].
- [33] CMS collaboration, *The CMS Experiment at the CERN LHC*, 2008 *JINST* **3** S08004 [[INSPIRE](#)].

- [34] CMS collaboration, *The CMS trigger system*, [2017 JINST 12 P01020](#) [[arXiv:1609.02366](#)] [[INSPIRE](#)].
- [35] P. Nason, *A New method for combining NLO QCD with shower Monte Carlo algorithms*, [JHEP 11 \(2004\) 040](#) [[hep-ph/0409146](#)] [[INSPIRE](#)].
- [36] S. Frixione, P. Nason and C. Oleari, *Matching NLO QCD computations with Parton Shower simulations: the POWHEG method*, [JHEP 11 \(2007\) 070](#) [[arXiv:0709.2092](#)] [[INSPIRE](#)].
- [37] S. Alioli, P. Nason, C. Oleari and E. Re, *A general framework for implementing NLO calculations in shower Monte Carlo programs: the POWHEG BOX*, [JHEP 06 \(2010\) 043](#) [[arXiv:1002.2581](#)] [[INSPIRE](#)].
- [38] E. Bagnaschi, G. Degrossi, P. Slavich and A. Vicini, *Higgs production via gluon fusion in the POWHEG approach in the SM and in the MSSM*, [JHEP 02 \(2012\) 088](#) [[arXiv:1111.2854](#)] [[INSPIRE](#)].
- [39] P. Nason and C. Oleari, *NLO Higgs boson production via vector-boson fusion matched with shower in POWHEG*, [JHEP 02 \(2010\) 037](#) [[arXiv:0911.5299](#)] [[INSPIRE](#)].
- [40] Y. Gao, A.V. Gritsan, Z. Guo, K. Melnikov, M. Schulze and N.V. Tran, *Spin Determination of Single-Produced Resonances at Hadron Colliders*, [Phys. Rev. D 81 \(2010\) 075022](#) [[arXiv:1001.3396](#)] [[INSPIRE](#)].
- [41] S. Bolognesi et al., *On the spin and parity of a single-produced resonance at the LHC*, [Phys. Rev. D 86 \(2012\) 095031](#) [[arXiv:1208.4018](#)] [[INSPIRE](#)].
- [42] LHC HIGGS CROSS SECTION Working Group, *Handbook of LHC Higgs Cross Sections: 4. Deciphering the Nature of the Higgs Sector*, [CERN Yellow Rep. Monogr. 2 \(2017\) 1](#) [[arXiv:1610.07922](#)] [[INSPIRE](#)].
- [43] J. Alwall et al., *The automated computation of tree-level and next-to-leading order differential cross sections and their matching to parton shower simulations*, [JHEP 07 \(2014\) 079](#) [[arXiv:1405.0301](#)] [[INSPIRE](#)].
- [44] R. Frederix and S. Frixione, *Merging meets matching in MC@NLO*, [JHEP 12 \(2012\) 061](#) [[arXiv:1209.6215](#)] [[INSPIRE](#)].
- [45] Y. Li and F. Petriello, *Combining QCD and electroweak corrections to dilepton production in FEWZ*, [Phys. Rev. D 86 \(2012\) 094034](#) [[arXiv:1208.5967](#)] [[INSPIRE](#)].
- [46] E. Re, *Single-top Wt -channel production matched with parton showers using the POWHEG method*, [Eur. Phys. J. C 71 \(2011\) 1547](#) [[arXiv:1009.2450](#)] [[INSPIRE](#)].
- [47] S. Frixione, P. Nason and G. Ridolfi, *A Positive-weight next-to-leading-order Monte Carlo for heavy flavour hadroproduction*, [JHEP 09 \(2007\) 126](#) [[arXiv:0707.3088](#)] [[INSPIRE](#)].
- [48] P. Kant et al., *HatHor for single top-quark production: Updated predictions and uncertainty estimates for single top-quark production in hadronic collisions*, [Comput. Phys. Commun. 191 \(2015\) 74](#) [[arXiv:1406.4403](#)] [[INSPIRE](#)].
- [49] M. Czakon and A. Mitov, *Top++: A Program for the Calculation of the Top-Pair Cross-Section at Hadron Colliders*, [Comput. Phys. Commun. 185 \(2014\) 2930](#) [[arXiv:1112.5675](#)] [[INSPIRE](#)].
- [50] T. Melia, P. Nason, R. Röntsch and G. Zanderighi, *W^+W^- , WZ and ZZ production in the POWHEG BOX*, [JHEP 11 \(2011\) 078](#) [[arXiv:1107.5051](#)] [[INSPIRE](#)].

- [51] J.M. Campbell, R.K. Ellis and C. Williams, *Bounding the Higgs Width at the LHC: Complementary Results from $H \rightarrow WW$* , *Phys. Rev. D* **89** (2014) 053011 [[arXiv:1312.1628](#)] [[INSPIRE](#)].
- [52] T. Gehrmann et al., *W^+W^- Production at Hadron Colliders in Next to Next to Leading Order QCD*, *Phys. Rev. Lett.* **113** (2014) 212001 [[arXiv:1408.5243](#)] [[INSPIRE](#)].
- [53] F. Caola, K. Melnikov, R. Röntsch and L. Tancredi, *QCD corrections to W^+W^- production through gluon fusion*, *Phys. Lett. B* **754** (2016) 275 [[arXiv:1511.08617](#)] [[INSPIRE](#)].
- [54] P. Meade, H. Ramani and M. Zeng, *Transverse momentum resummation effects in W^+W^- measurements*, *Phys. Rev. D* **90** (2014) 114006 [[arXiv:1407.4481](#)] [[INSPIRE](#)].
- [55] P. Jaiswal and T. Okui, *Explanation of the WW excess at the LHC by jet-veto resummation*, *Phys. Rev. D* **90** (2014) 073009 [[arXiv:1407.4537](#)] [[INSPIRE](#)].
- [56] T. Sjöstrand et al., *An Introduction to PYTHIA 8.2*, *Comput. Phys. Commun.* **191** (2015) 159 [[arXiv:1410.3012](#)] [[INSPIRE](#)].
- [57] NNPDF collaboration, *Parton distributions with QED corrections*, *Nucl. Phys. B* **877** (2013) 290 [[arXiv:1308.0598](#)] [[INSPIRE](#)].
- [58] NNPDF collaboration, *Unbiased global determination of parton distributions and their uncertainties at NNLO and at LO*, *Nucl. Phys. B* **855** (2012) 153 [[arXiv:1107.2652](#)] [[INSPIRE](#)].
- [59] CMS collaboration, *Event generator tunes obtained from underlying event and multiparton scattering measurements*, *Eur. Phys. J. C* **76** (2016) 155 [[arXiv:1512.00815](#)] [[INSPIRE](#)].
- [60] P. Richardson and A. Wilcock, *Monte Carlo Simulation of Hard Radiation in Decays in Beyond the Standard Model Physics in HERWIG++*, *Eur. Phys. J. C* **74** (2014) 2713 [[arXiv:1303.4563](#)] [[INSPIRE](#)].
- [61] M. Bähr et al., *HERWIG++ Physics and Manual*, *Eur. Phys. J. C* **58** (2008) 639 [[arXiv:0803.0883](#)] [[INSPIRE](#)].
- [62] GEANT4 collaboration, *GEANT4: A Simulation toolkit*, *Nucl. Instrum. Meth. A* **506** (2003) 250 [[INSPIRE](#)].
- [63] CMS collaboration, *Particle-flow reconstruction and global event description with the CMS detector*, *2017 JINST* **12** P10003 [[arXiv:1706.04965](#)] [[INSPIRE](#)].
- [64] M. Cacciari, G.P. Salam and G. Soyez, *The anti- k_t jet clustering algorithm*, *JHEP* **04** (2008) 063 [[arXiv:0802.1189](#)] [[INSPIRE](#)].
- [65] M. Cacciari, G.P. Salam and G. Soyez, *FastJet User Manual*, *Eur. Phys. J. C* **72** (2012) 1896 [[arXiv:1111.6097](#)] [[INSPIRE](#)].
- [66] CMS collaboration, *Performance of Electron Reconstruction and Selection with the CMS Detector in Proton-Proton Collisions at $\sqrt{s} = 8$ TeV*, *2015 JINST* **10** P06005 [[arXiv:1502.02701](#)] [[INSPIRE](#)].
- [67] CMS collaboration, *Performance of the CMS muon detector and muon reconstruction with proton-proton collisions at $\sqrt{s} = 13$ TeV*, *2018 JINST* **13** P06015 [[arXiv:1804.04528](#)] [[INSPIRE](#)].
- [68] M. Cacciari and G.P. Salam, *Pileup subtraction using jet areas*, *Phys. Lett. B* **659** (2008) 119 [[arXiv:0707.1378](#)] [[INSPIRE](#)].

- [69] CMS collaboration, *Determination of Jet Energy Calibration and Transverse Momentum Resolution in CMS*, **2011 JINST** **6** P11002 [[arXiv:1107.4277](#)] [[INSPIRE](#)].
- [70] D. Bertolini, P. Harris, M. Low and N. Tran, *Pileup Per Particle Identification*, **JHEP** **10** (2014) 059 [[arXiv:1407.6013](#)] [[INSPIRE](#)].
- [71] M. Dasgupta, A. Fregoso, S. Marzani and G.P. Salam, *Towards an understanding of jet substructure*, **JHEP** **09** (2013) 029 [[arXiv:1307.0007](#)] [[INSPIRE](#)].
- [72] J.M. Butterworth, A.R. Davison, M. Rubin and G.P. Salam, *Jet substructure as a new Higgs search channel at the LHC*, **Phys. Rev. Lett.** **100** (2008) 242001 [[arXiv:0802.2470](#)] [[INSPIRE](#)].
- [73] A.J. Larkoski, S. Marzani, G. Soyez and J. Thaler, *Soft Drop*, **JHEP** **05** (2014) 146 [[arXiv:1402.2657](#)] [[INSPIRE](#)].
- [74] J. Thaler and K. Van Tilburg, *Identifying Boosted Objects with N -subjettiness*, **JHEP** **03** (2011) 015 [[arXiv:1011.2268](#)] [[INSPIRE](#)].
- [75] CMS collaboration, *Identification of heavy-flavour jets with the CMS detector in pp collisions at 13 TeV*, **2018 JINST** **13** P05011 [[arXiv:1712.07158](#)] [[INSPIRE](#)].
- [76] N. Craig, F. D’Eramo, P. Draper, S. Thomas and H. Zhang, *The Hunt for the Rest of the Higgs Bosons*, **JHEP** **06** (2015) 137 [[arXiv:1504.04630](#)] [[INSPIRE](#)].
- [77] D. Chowdhury and O. Eberhardt, *Update of Global Two-Higgs-Doublet Model Fits*, **JHEP** **05** (2018) 161 [[arXiv:1711.02095](#)] [[INSPIRE](#)].
- [78] P. Fayet, *Supergauge Invariant Extension of the Higgs Mechanism and a Model for the electron and Its Neutrino*, **Nucl. Phys. B** **90** (1975) 104 [[INSPIRE](#)].
- [79] P. Fayet, *Spontaneously Broken Supersymmetric Theories of Weak, Electromagnetic and Strong Interactions*, **Phys. Lett. B** **69** (1977) 489 [[INSPIRE](#)].
- [80] M. Carena, S. Heinemeyer, O. Stål, C.E.M. Wagner and G. Weiglein, *MSSM Higgs Boson Searches at the LHC: Benchmark Scenarios after the Discovery of a Higgs-like Particle*, **Eur. Phys. J. C** **73** (2013) 2552 [[arXiv:1302.7033](#)] [[INSPIRE](#)].
- [81] A. Djouadi and J. Quevillon, *The MSSM Higgs sector at a high M_{SUSY} : reopening the low $\tan\beta$ regime and heavy Higgs searches*, **JHEP** **10** (2013) 028 [[arXiv:1304.1787](#)] [[INSPIRE](#)].
- [82] L. Maiani, A.D. Polosa and V. Riquer, *Bounds to the Higgs Sector Masses in Minimal Supersymmetry from LHC Data*, **Phys. Lett. B** **724** (2013) 274 [[arXiv:1305.2172](#)] [[INSPIRE](#)].
- [83] A. Djouadi, L. Maiani, G. Moreau, A. Polosa, J. Quevillon and V. Riquer, *The post-Higgs MSSM scenario: Habemus MSSM?*, **Eur. Phys. J. C** **73** (2013) 2650 [[arXiv:1307.5205](#)] [[INSPIRE](#)].
- [84] A. Djouadi, L. Maiani, A. Polosa, J. Quevillon and V. Riquer, *Fully covering the MSSM Higgs sector at the LHC*, **JHEP** **06** (2015) 168 [[arXiv:1502.05653](#)] [[INSPIRE](#)].
- [85] E. Bagnaschi et al., *MSSM Higgs Boson Searches at the LHC: Benchmark Scenarios for Run 2 and Beyond*, **Eur. Phys. J. C** **79** (2019) 617 [[arXiv:1808.07542](#)] [[INSPIRE](#)].
- [86] R.V. Harlander, S. Liebler and H. Mantler, *SusHi: A program for the calculation of Higgs production in gluon fusion and bottom-quark annihilation in the Standard Model and the MSSM*, **Comput. Phys. Commun.** **184** (2013) 1605 [[arXiv:1212.3249](#)] [[INSPIRE](#)].

- [87] R.V. Harlander, S. Liebler and H. Mantler, *SusHi Bento: Beyond NNLO and the heavy-top limit*, *Comput. Phys. Commun.* **212** (2017) 239 [[arXiv:1605.03190](#)] [[INSPIRE](#)].
- [88] M. Spira, A. Djouadi, D. Graudenz and P.M. Zerwas, *Higgs boson production at the LHC*, *Nucl. Phys. B* **453** (1995) 17 [[hep-ph/9504378](#)] [[INSPIRE](#)].
- [89] R.V. Harlander and W.B. Kilgore, *Next-to-next-to-leading order Higgs production at hadron colliders*, *Phys. Rev. Lett.* **88** (2002) 201801 [[hep-ph/0201206](#)] [[INSPIRE](#)].
- [90] C. Anastasiou and K. Melnikov, *Higgs boson production at hadron colliders in NNLO QCD*, *Nucl. Phys. B* **646** (2002) 220 [[hep-ph/0207004](#)] [[INSPIRE](#)].
- [91] V. Ravindran, J. Smith and W.L. van Neerven, *NNLO corrections to the total cross-section for Higgs boson production in hadron hadron collisions*, *Nucl. Phys. B* **665** (2003) 325 [[hep-ph/0302135](#)] [[INSPIRE](#)].
- [92] U. Aglietti, R. Bonciani, G. Degrossi and A. Vicini, *Two loop light fermion contribution to Higgs production and decays*, *Phys. Lett. B* **595** (2004) 432 [[hep-ph/0404071](#)] [[INSPIRE](#)].
- [93] R. Bonciani, G. Degrossi and A. Vicini, *On the Generalized Harmonic Polylogarithms of One Complex Variable*, *Comput. Phys. Commun.* **182** (2011) 1253 [[arXiv:1007.1891](#)] [[INSPIRE](#)].
- [94] R.V. Harlander and M. Steinhauser, *Supersymmetric Higgs production in gluon fusion at next-to-leading order*, *JHEP* **09** (2004) 066 [[hep-ph/0409010](#)] [[INSPIRE](#)].
- [95] R. Harlander and P. Kant, *Higgs production and decay: Analytic results at next-to-leading order QCD*, *JHEP* **12** (2005) 015 [[hep-ph/0509189](#)] [[INSPIRE](#)].
- [96] G. Degrossi and P. Slavich, *NLO QCD bottom corrections to Higgs boson production in the MSSM*, *JHEP* **11** (2010) 044 [[arXiv:1007.3465](#)] [[INSPIRE](#)].
- [97] G. Degrossi, S. Di Vita and P. Slavich, *On the NLO QCD Corrections to the Production of the Heaviest Neutral Higgs Scalar in the MSSM*, *Eur. Phys. J. C* **72** (2012) 2032 [[arXiv:1204.1016](#)] [[INSPIRE](#)].
- [98] S. Heinemeyer, W. Hollik and G. Weiglein, *FeynHiggs: A Program for the calculation of the masses of the neutral CP even Higgs bosons in the MSSM*, *Comput. Phys. Commun.* **124** (2000) 76 [[hep-ph/9812320](#)] [[INSPIRE](#)].
- [99] S. Heinemeyer, W. Hollik and G. Weiglein, *The Masses of the neutral CP-even Higgs bosons in the MSSM: Accurate analysis at the two loop level*, *Eur. Phys. J. C* **9** (1999) 343 [[hep-ph/9812472](#)] [[INSPIRE](#)].
- [100] G. Degrossi, S. Heinemeyer, W. Hollik, P. Slavich and G. Weiglein, *Towards high precision predictions for the MSSM Higgs sector*, *Eur. Phys. J. C* **28** (2003) 133 [[hep-ph/0212020](#)] [[INSPIRE](#)].
- [101] M. Frank, T. Hahn, S. Heinemeyer, W. Hollik, H. Rzehak and G. Weiglein, *The Higgs Boson Masses and Mixings of the Complex MSSM in the Feynman-Diagrammatic Approach*, *JHEP* **02** (2007) 047 [[hep-ph/0611326](#)] [[INSPIRE](#)].
- [102] T. Hahn, S. Heinemeyer, W. Hollik, H. Rzehak and G. Weiglein, *High-Precision Predictions for the Light CP-Even Higgs Boson Mass of the Minimal Supersymmetric Standard Model*, *Phys. Rev. Lett.* **112** (2014) 141801 [[arXiv:1312.4937](#)] [[INSPIRE](#)].
- [103] H. Bahl and W. Hollik, *Precise prediction for the light MSSM Higgs boson mass combining effective field theory and fixed-order calculations*, *Eur. Phys. J. C* **76** (2016) 499 [[arXiv:1608.01880](#)] [[INSPIRE](#)].

- [104] H. Bahl, S. Heinemeyer, W. Hollik and G. Weiglein, *Reconciling EFT and hybrid calculations of the light MSSM Higgs-boson mass*, *Eur. Phys. J. C* **78** (2018) 57 [[arXiv:1706.00346](#)] [[INSPIRE](#)].
- [105] A. Djouadi, J. Kalinowski and M. Spira, *HDECAY: A Program for Higgs boson decays in the standard model and its supersymmetric extension*, *Comput. Phys. Commun.* **108** (1998) 56 [[hep-ph/9704448](#)] [[INSPIRE](#)].
- [106] M.M. Mühlleitner, A. Djouadi and M. Spira, *Decays of supersymmetric particles: The Program SUSY-HIT (SUspect-SdecaY-HDECAY-InTerface)*, *Acta Phys. Polon.* **B 38** (2007) 635 [[hep-ph/0609292](#)] [[INSPIRE](#)].
- [107] A. Djouadi, J. Kalinowski, M.M. Mühlleitner and M. Spira, *HDECAY: Twenty++ years after*, *Comput. Phys. Commun.* **238** (2019) 214 [[arXiv:1801.09506](#)] [[INSPIRE](#)].
- [108] A. Bredenstein, A. Denner, S. Dittmaier and M.M. Weber, *Precise predictions for the Higgs-boson decay $H \rightarrow WW/ZZ \rightarrow 4$ leptons*, *Phys. Rev. D* **74** (2006) 013004 [[hep-ph/0604011](#)] [[INSPIRE](#)].
- [109] A. Bredenstein, A. Denner, S. Dittmaier and M.M. Weber, *Radiative corrections to the semileptonic and hadronic Higgs-boson decays $H \rightarrow WW/ZZ \rightarrow 4$ fermions*, *JHEP* **02** (2007) 080 [[hep-ph/0611234](#)] [[INSPIRE](#)].
- [110] D. Eriksson, J. Rathsmann and O. Stål, *2HDMC: Two-Higgs-Doublet Model Calculator Physics and Manual*, *Comput. Phys. Commun.* **181** (2010) 189 [[arXiv:0902.0851](#)] [[INSPIRE](#)].
- [111] M. Spira, *HIGLU: A program for the calculation of the total Higgs production cross-section at hadron colliders via gluon fusion including QCD corrections*, [hep-ph/9510347](#) [[INSPIRE](#)].
- [112] R. Harlander, M.M. Mühlleitner, J. Rathsmann, M. Spira and O. Stål, *Interim recommendations for the evaluation of Higgs production cross sections and branching ratios at the LHC in the Two-Higgs-Doublet Model*, [arXiv:1312.5571](#) [[INSPIRE](#)].
- [113] D0 collaboration, *Direct measurement of the top quark mass at DO collaboration*, *Phys. Rev. D* **58** (1998) 052001 [[hep-ex/9801025](#)] [[INSPIRE](#)].
- [114] CMS collaboration, *Measurement of the Inclusive W and Z Production Cross Sections in pp Collisions at $\sqrt{s} = 7$ TeV*, *JHEP* **10** (2011) 132 [[arXiv:1107.4789](#)] [[INSPIRE](#)].
- [115] CMS collaboration, *Identification of b-Quark Jets with the CMS Experiment*, *2013 JINST* **8** P04013 [[arXiv:1211.4462](#)] [[INSPIRE](#)].
- [116] CMS collaboration, *Identification techniques for highly boosted W bosons that decay into hadrons*, *JHEP* **12** (2014) 017 [[arXiv:1410.4227](#)] [[INSPIRE](#)].
- [117] T. Junk, *Confidence level computation for combining searches with small statistics*, *Nucl. Instrum. Meth. A* **434** (1999) 435 [[hep-ex/9902006](#)] [[INSPIRE](#)].
- [118] A.L. Read, *Presentation of search results: The CL_s technique*, *J. Phys. G* **28** (2002) 2693 [[INSPIRE](#)].
- [119] G. Cowan, K. Cranmer, E. Gross and O. Vitells, *Asymptotic formulae for likelihood-based tests of new physics*, *Eur. Phys. J. C* **71** (2011) 1554 [Erratum *ibid.* **C 73** (2013) 2501] [[arXiv:1007.1727](#)] [[INSPIRE](#)].
- [120] R.J. Barlow and C. Beeston, *Fitting using finite Monte Carlo samples*, *Comput. Phys. Commun.* **77** (1993) 219 [[INSPIRE](#)].

- [121] J.M. Butterworth et al., *PDF4LHC recommendations for LHC Run II*, *J. Phys. G* **43** (2016) 023001 [[arXiv:1510.03865](#)] [[INSPIRE](#)].
- [122] M. Cacciari, S. Frixione, M.L. Mangano, P. Nason and G. Ridolfi, *The $t\bar{t}$ cross-section at 1.8 TeV and 1.96 TeV: A Study of the systematics due to parton densities and scale dependence*, *JHEP* **04** (2004) 068 [[hep-ph/0303085](#)] [[INSPIRE](#)].
- [123] CMS collaboration, *CMS Luminosity Measurements for the 2016 Data Taking Period*, *CMS-PAS-LUM-17-001* (2017) [[INSPIRE](#)].
- [124] R. Boughezal, X. Liu, F. Petriello, F.J. Tackmann and J.R. Walsh, *Combining Resummed Higgs Predictions Across Jet Bins*, *Phys. Rev. D* **89** (2014) 074044 [[arXiv:1312.4535](#)] [[INSPIRE](#)].
- [125] CMS collaboration, *Measurements of the $pp \rightarrow WZ$ inclusive and differential production cross section and constraints on charged anomalous triple gauge couplings at $\sqrt{s} = 13$ TeV*, *JHEP* **04** (2019) 122 [[arXiv:1901.03428](#)] [[INSPIRE](#)].
- [126] CMS collaboration, *Measurement of differential cross sections for Z boson production in association with jets in proton-proton collisions at $\sqrt{s} = 13$ TeV*, *Eur. Phys. J. C* **78** (2018) 965 [[arXiv:1804.05252](#)] [[INSPIRE](#)].
- [127] ATLAS collaboration, *Search for Minimal Supersymmetric Standard Model Higgs bosons H/A and for a Z' boson in the $\tau\tau$ final state produced in pp collisions at $\sqrt{s} = 13$ TeV with the ATLAS Detector*, *Eur. Phys. J. C* **76** (2016) 585 [[arXiv:1608.00890](#)] [[INSPIRE](#)].
- [128] CMS collaboration, *Search for additional neutral MSSM Higgs bosons in the $\tau\tau$ final state in proton-proton collisions at $\sqrt{s} = 13$ TeV*, *JHEP* **09** (2018) 007 [[arXiv:1803.06553](#)] [[INSPIRE](#)].

The CMS collaboration

Yerevan Physics Institute, Yerevan, Armenia

A.M. Sirunyan[†], A. Tumasyan

Institut für Hochenergiephysik, Wien, Austria

W. Adam, F. Ambrogio, T. Bergauer, J. Brandstetter, M. Dragicevic, J. Erö, A. Escalante Del Valle, M. Flechl, R. Frühwirth¹, M. Jeitler¹, N. Krammer, I. Krätschmer, D. Liko, T. Madlener, I. Mikulec, N. Rad, J. Schieck¹, R. Schöffbeck, M. Spanring, D. Spitzbart, W. Waltenberger, C.-E. Wulz¹, M. Zarucki

Institute for Nuclear Problems, Minsk, Belarus

V. Drugakov, V. Mossolov, J. Suarez Gonzalez

Universiteit Antwerpen, Antwerpen, Belgium

M.R. Darwish, E.A. De Wolf, D. Di Croce, X. Janssen, J. Lauwers, A. Lelek, M. Pieters, H. Rejeb Sfar, H. Van Haevermaet, P. Van Mechelen, S. Van Putte, N. Van Remortel

Vrije Universiteit Brussel, Brussel, Belgium

F. Blekman, E.S. Bols, S.S. Chhibra, J. D'Hondt, J. De Clercq, D. Lontkovskyi, S. Lowette, I. Marchesini, S. Moortgat, L. Moreels, Q. Python, K. Skovpen, S. Tavernier, W. Van Doninck, P. Van Mulders, I. Van Parijs

Université Libre de Bruxelles, Bruxelles, Belgium

D. Beghin, B. Bilin, H. Brun, B. Clerbaux, G. De Lentdecker, H. Delannoy, B. Dorney, L. Favart, A. Grebenyuk, A.K. Kalsi, J. Luetic, A. Popov, N. Postiau, E. Starling, L. Thomas, C. Vander Velde, P. Vanlaer, D. Vannerom

Ghent University, Ghent, Belgium

T. Cornelis, D. Dobur, I. Khvastunov², M. Niedziela, C. Roskas, D. Trocino, M. Tytgat, W. Verbeke, B. Vermassen, M. Vit, N. Zaganidis

Université Catholique de Louvain, Louvain-la-Neuve, Belgium

O. Bondu, G. Bruno, C. Caputo, P. David, C. Delaere, M. Delcourt, A. Giammanco, V. Lemaitre, A. Magitteri, J. Prisciandaro, A. Saggio, M. Vidal Marono, P. Vischia, J. Zobec

Centro Brasileiro de Pesquisas Fisicas, Rio de Janeiro, Brazil

F.L. Alves, G.A. Alves, G. Correia Silva, C. Hensel, A. Moraes, P. Rebello Teles

Universidade do Estado do Rio de Janeiro, Rio de Janeiro, Brazil

E. Belchior Batista Das Chagas, W. Carvalho, J. Chinellato³, E. Coelho, E.M. Da Costa, G.G. Da Silveira⁴, D. De Jesus Damiao, C. De Oliveira Martins, S. Fonseca De Souza, L.M. Huertas Guativa, H. Malbouisson, J. Martins⁵, D. Matos Figueiredo, M. Medina Jaime⁶, M. Melo De Almeida, C. Mora Herrera, L. Mundim, H. Nogima, W.L. Prado Da Silva, L.J. Sanchez Rosas, A. Santoro, A. Sznajder, M. Thiel, E.J. Tonelli Manganote³, F. Torres Da Silva De Araujo, A. Vilela Pereira

Universidade Estadual Paulista^a, Universidade Federal do ABC^b, São Paulo, Brazil

S. Ahuja^a, C.A. Bernardes^a, L. Calligaris^a, T.R. Fernandez Perez Tomei^a, E.M. Gregores^b, D.S. Lemos, P.G. Mercadante^b, S.F. Novaes^a, SandraS. Padula^a

Institute for Nuclear Research and Nuclear Energy, Bulgarian Academy of Sciences, Sofia, Bulgaria

A. Aleksandrov, G. Antchev, R. Hadjiiska, P. Iaydjiev, A. Marinov, M. Misheva, M. Rodozov, M. Shopova, G. Sultanov

University of Sofia, Sofia, Bulgaria

M. Bonchev, A. Dimitrov, T. Ivanov, L. Litov, B. Pavlov, P. Petkov

Beihang University, Beijing, China

W. Fang⁷, X. Gao⁷, L. Yuan

Institute of High Energy Physics, Beijing, China

M. Ahmad, G.M. Chen, H.S. Chen, M. Chen, C.H. Jiang, D. Leggat, H. Liao, Z. Liu, S.M. Shaheen⁸, A. Spiezia, J. Tao, E. Yazgan, H. Zhang, S. Zhang⁸, J. Zhao

State Key Laboratory of Nuclear Physics and Technology, Peking University, Beijing, China

A. Agapitos, Y. Ban, G. Chen, A. Levin, J. Li, L. Li, Q. Li, Y. Mao, S.J. Qian, D. Wang, Q. Wang

Tsinghua University, Beijing, China

Z. Hu, Y. Wang

Universidad de Los Andes, Bogota, Colombia

C. Avila, A. Cabrera, L.F. Chaparro Sierra, C. Florez, C.F. González Hernández, M.A. Segura Delgado

Universidad de Antioquia, Medellin, Colombia

J. Mejia Guisao, J.D. Ruiz Alvarez, C.A. Salazar González, N. Vanegas Arbelaez

University of Split, Faculty of Electrical Engineering, Mechanical Engineering and Naval Architecture, Split, Croatia

D. Giljanović, N. Godinovic, D. Lelas, I. Puljak, T. Sculac

University of Split, Faculty of Science, Split, Croatia

Z. Antunovic, M. Kovac

Institute Rudjer Boskovic, Zagreb, Croatia

V. Brigljevic, S. Ceci, D. Ferencek, K. Kadija, B. Mesic, M. Roguljic, A. Starodumov⁹, T. Susa

University of Cyprus, Nicosia, Cyprus

M.W. Ather, A. Attikis, E. Erodotou, A. Ioannou, M. Kolosova, S. Konstantinou, G. Mavromanolakis, J. Mousa, C. Nicolaou, F. Ptochos, P.A. Razis, H. Rykaczewski, D. Tsiakkouri

Charles University, Prague, Czech Republic

M. Finger¹⁰, M. Finger Jr.¹⁰, A. Kveton, J. Tomsa

Escuela Politecnica Nacional, Quito, Ecuador

E. Ayala

Universidad San Francisco de Quito, Quito, Ecuador

E. Carrera Jarrin

**Academy of Scientific Research and Technology of the Arab Republic of Egypt,
Egyptian Network of High Energy Physics, Cairo, Egypt**

H. Abdalla¹¹, E. Salama^{12,13}

National Institute of Chemical Physics and Biophysics, Tallinn, Estonia

S. Bhowmik, A. Carvalho Antunes De Oliveira, R.K. Dewanjee, K. Ehataht, M. Kadastik,
M. Raidal, C. Veelken

Department of Physics, University of Helsinki, Helsinki, Finland

P. Eerola, L. Forthomme, H. Kirschenmann, K. Osterberg, M. Voutilainen

Helsinki Institute of Physics, Helsinki, Finland

F. Garcia, J. Havukainen, J.K. Heikkilä, T. Järvinen, V. Karimäki, R. Kinnunen,
T. Lampén, K. Lassila-Perini, S. Laurila, S. Lehti, T. Lindén, P. Luukka, T. Mäenpää,
H. Siikonen, E. Tuominen, J. Tuominiemi

Lappeenranta University of Technology, Lappeenranta, Finland

T. Tuuva

IRFU, CEA, Université Paris-Saclay, Gif-sur-Yvette, France

M. Besancon, F. Couderc, M. Dejardin, D. Denegri, B. Fabbro, J.L. Faure, F. Ferri,
S. Ganjour, A. Givernaud, P. Gras, G. Hamel de Monchenault, P. Jarry, C. Leloup, E. Locci,
J. Malcles, J. Rander, A. Rosowsky, M.Ö. Sahin, A. Savoy-Navarro¹⁴, M. Titov

**Laboratoire Leprince-Ringuet, CNRS/IN2P3, Ecole Polytechnique, Institut
Polytechnique de Paris**

C. Amendola, F. Beaudette, P. Busson, C. Charlot, B. Diab, G. Falmagne,
R. Granier de Cassagnac, I. Kucher, A. Lobanov, C. Martin Perez, M. Nguyen, C. Ochando,
P. Paganini, J. Rembser, R. Salerno, J.B. Sauvan, Y. Sirois, A. Zabi, A. Zghiche

Université de Strasbourg, CNRS, IPHC UMR 7178, Strasbourg, France

J.-L. Agram¹⁵, J. Andrea, D. Bloch, G. Bourgatte, J.-M. Brom, E.C. Chabert, C. Collard,
E. Conte¹⁵, J.-C. Fontaine¹⁵, D. Gelé, U. Goerlach, M. Jansová, A.-C. Le Bihan, N. Tonon,
P. Van Hove

**Centre de Calcul de l'Institut National de Physique Nucleaire et de Physique
des Particules, CNRS/IN2P3, Villeurbanne, France**

S. Gadrat

Université de Lyon, Université Claude Bernard Lyon 1, CNRS-IN2P3, Institut de Physique Nucléaire de Lyon, Villeurbanne, France

S. Beauceron, C. Bernet, G. Boudoul, C. Camen, N. Chanon, R. Chierici, D. Contardo, P. Depasse, H. El Mamouni, J. Fay, S. Gascon, M. Gouzevitch, B. Ille, Sa. Jain, F. Lagarde, I.B. Laktineh, H. Lattaud, M. Lethuillier, L. Mirabito, S. Perries, V. Sordini, G. Touquet, M. Vander Donckt, S. Viret

Georgian Technical University, Tbilisi, Georgia

T. Toriashvili¹⁶

Tbilisi State University, Tbilisi, Georgia

Z. Tsamalaidze¹⁰

RWTH Aachen University, I. Physikalisches Institut, Aachen, Germany

C. Autermann, L. Feld, M.K. Kiesel, K. Klein, M. Lipinski, D. Meuser, A. Pauls, M. Preuten, M.P. Rauch, C. Schomakers, J. Schulz, M. Teroerde, B. Wittmer

RWTH Aachen University, III. Physikalisches Institut A, Aachen, Germany

A. Albert, M. Erdmann, S. Erdweg, T. Esch, B. Fischer, R. Fischer, S. Ghosh, T. Hebbeker, K. Hoepfner, H. Keller, L. Mastrolorenzo, M. Merschmeyer, A. Meyer, P. Millet, G. Mo-cellin, S. Mondal, S. Mukherjee, D. Noll, A. Novak, T. Pook, A. Pozdnyakov, T. Quast, M. Radziej, Y. Rath, H. Reithler, M. Rieger, J. Roemer, A. Schmidt, S.C. Schuler, A. Sharma, S. Thüer, S. Wiedenbeck

RWTH Aachen University, III. Physikalisches Institut B, Aachen, Germany

G. Flügge, W. Haj Ahmad¹⁷, O. Hlushchenko, T. Kress, T. Müller, A. Nehrkorn, A. Nowack, C. Pistone, O. Pooth, D. Roy, H. Sert, A. Stahl¹⁸

Deutsches Elektronen-Synchrotron, Hamburg, Germany

M. Aldaya Martin, P. Asmuss, I. Babounikau, H. Bakhshiansohi, K. Beernaert, O. Behnke, U. Behrens, A. Bermúdez Martínez, D. Bertsche, A.A. Bin Anuar, K. Borrás¹⁹, V. Botta, A. Campbell, A. Cardini, P. Connor, S. Consuegra Rodríguez, C. Contreras-Campana, V. Danilov, A. De Wit, M.M. Defranchis, C. Diez Pardos, D. Domínguez Damiani, G. Eckerlin, D. Eckstein, T. Eichhorn, A. Elwood, E. Eren, E. Gallo²⁰, A. Geiser, J.M. Grados Luyando, A. Grohsjean, M. Guthoff, M. Haranko, A. Harb, A. Jafari, N.Z. Jomhari, H. Jung, A. Kasem¹⁹, M. Kasemann, H. Kaveh, J. Keaveney, C. Kleinwort, J. Knolle, D. Krücker, W. Lange, T. Lenz, J. Leonard, J. Lidrych, K. Lipka, W. Lohmann²¹, R. Mankel, I.-A. Melzer-Pellmann, A.B. Meyer, M. Meyer, M. Missiroli, G. Mittag, J. Mnich, A. Mussgiller, V. Myronenko, D. Pérez Adán, S.K. Pflitsch, D. Pitzl, A. Raspereza, A. Saibel, M. Savitskyi, V. Scheurer, P. Schütze, C. Schwanenberger, R. Shevchenko, A. Singh, H. Tholen, O. Turkot, A. Vagnerini, M. Van De Klundert, G.P. Van Onsem, R. Walsh, Y. Wen, K. Wichmann, C. Wissing, O. Zenaiev, R. Zlebick

University of Hamburg, Hamburg, Germany

R. Aggleton, S. Bein, L. Benato, A. Benecke, V. Blobel, T. Dreyer, A. Ebrahimi, A. Fröhlich, C. Garbers, E. Garutti, D. Gonzalez, P. Gunnellini, J. Haller, A. Hinzmann, A. Karavdina, G. Kasieczka, R. Klanner, R. Kogler, N. Kovalchuk, S. Kurz, V. Kutzner,

J. Lange, T. Lange, A. Malara, D. Marconi, J. Multhaupt, C.E.N. Niemeyer, D. Nowatschin, A. Perieanu, A. Reimers, O. Rieger, C. Scharf, P. Schleper, S. Schumann, J. Schwandt, J. Sonneveld, H. Stadie, G. Steinbrück, F.M. Stober, M. Stöver, B. Vormwald, I. Zoi

Karlsruher Institut fuer Technologie, Karlsruhe, Germany

M. Akbiyik, C. Barth, M. Baselga, S. Baur, T. Berger, E. Butz, R. Caspart, T. Chwalek, W. De Boer, A. Dierlamm, K. El Morabit, N. Faltermann, M. Giffels, P. Goldenzweig, A. Gottmann, M.A. Harrendorf, F. Hartmann¹⁸, U. Husemann, S. Kudella, S. Mitra, M.U. Mozer, Th. Müller, M. Musich, A. Nürnberg, G. Quast, K. Rabbertz, M. Schröder, I. Shvetsov, H.J. Simonis, R. Ulrich, M. Weber, C. Wöhrmann, R. Wolf

Institute of Nuclear and Particle Physics (INPP), NCSR Demokritos, Aghia Paraskevi, Greece

G. Anagnostou, P. Asenov, G. Daskalakis, T. Geralis, A. Kyriakis, D. Loukas, G. Paspalaki

National and Kapodistrian University of Athens, Athens, Greece

M. Diamantopoulou, G. Karathanasis, P. Kontaxakis, A. Panagiotou, I. Papavergou, N. Saoulidou, A. Stakia, K. Theofilatos, K. Vellidis

National Technical University of Athens, Athens, Greece

G. Bakas, K. Kousouris, I. Papakrivopoulos, G. Tsipolitis

University of Ioánnina, Ioánnina, Greece

I. Evangelou, C. Foudas, P. Gianneios, P. Katsoulis, P. Kokkas, S. Mallios, K. Manitaras, N. Manthos, I. Papadopoulos, J. Strologas, F.A. Triantis, D. Tsitsonis

MTA-ELTE Lendület CMS Particle and Nuclear Physics Group, Eötvös Loránd University, Budapest, Hungary

M. Bartók²², M. Csanad, P. Major, K. Mandal, A. Mehta, M.I. Nagy, G. Pasztor, O. Surányi, G.I. Veres

Wigner Research Centre for Physics, Budapest, Hungary

G. Bencze, C. Hajdu, D. Horvath²³, F. Sikler, T.Á. Vámi, V. Veszpremi, G. Vesztergombi[†]

Institute of Nuclear Research ATOMKI, Debrecen, Hungary

N. Beni, S. Czellar, J. Karancsi²², A. Makovec, J. Molnar, Z. Szillasi

Institute of Physics, University of Debrecen, Debrecen, Hungary

P. Raics, D. Teyssier, Z.L. Trocsanyi, B. Ujvari

Eszterhazy Karoly University, Karoly Robert Campus, Gyongyos, Hungary

T. Csorgo, W.J. Metzger, F. Nemes, T. Novak

Indian Institute of Science (IISc), Bangalore, India

S. Choudhury, J.R. Komaragiri, P.C. Tiwari

National Institute of Science Education and Research, HBNI, Bhubaneswar, India

S. Bahinipati²⁵, C. Kar, G. Kole, P. Mal, V.K. Muraleedharan Nair Bindhu, A. Nayak²⁶, D.K. Sahoo²⁵, S.K. Swain

Panjab University, Chandigarh, India

S. Bansal, S.B. Beri, V. Bhatnagar, S. Chauhan, R. Chawla, N. Dhingra, R. Gupta, A. Kaur, M. Kaur, S. Kaur, P. Kumari, M. Lohan, M. Meena, K. Sandeep, S. Sharma, J.B. Singh, A.K. Viridi, G. Walia

University of Delhi, Delhi, India

A. Bhardwaj, B.C. Choudhary, R.B. Garg, M. Gola, S. Keshri, Ashok Kumar, S. Malhotra, M. Naimuddin, P. Priyanka, K. Ranjan, Aashaq Shah, R. Sharma

Saha Institute of Nuclear Physics, HBNI, Kolkata, India

R. Bhardwaj²⁷, M. Bharti²⁷, R. Bhattacharya, S. Bhattacharya, U. Bhawandeep²⁷, D. Bhowmik, S. Dey, S. Dutta, S. Ghosh, M. Maity²⁸, K. Mondal, S. Nandan, A. Purohit, P.K. Rout, G. Saha, S. Sarkar, T. Sarkar²⁸, M. Sharan, B. Singh²⁷, S. Thakur²⁷

Indian Institute of Technology Madras, Madras, India

P.K. Behera, P. Kalbhor, A. Muhammad, P.R. Pujahari, A. Sharma, A.K. Sikdar

Bhabha Atomic Research Centre, Mumbai, India

R. Chudasama, D. Dutta, V. Jha, V. Kumar, D.K. Mishra, P.K. Netrakanti, L.M. Pant, P. Shukla

Tata Institute of Fundamental Research-A, Mumbai, India

T. Aziz, M.A. Bhat, S. Dugad, G.B. Mohanty, N. Sur, RavindraKumar Verma

Tata Institute of Fundamental Research-B, Mumbai, India

S. Banerjee, S. Bhattacharya, S. Chatterjee, P. Das, M. Guchait, S. Karmakar, S. Kumar, G. Majumder, K. Mazumdar, N. Sahoo, S. Sawant

Indian Institute of Science Education and Research (IISER), Pune, India

S. Chauhan, S. Dube, V. Hegde, A. Kapoor, K. Kothekar, S. Pandey, A. Rane, A. Rastogi, S. Sharma

Institute for Research in Fundamental Sciences (IPM), Tehran, Iran

S. Chenarani²⁹, E. Eskandari Tadavani, S.M. Etesami²⁹, M. Khakzad, M. Mohammadi Najafabadi, M. Naseri, F. Rezaei Hosseinabadi

University College Dublin, Dublin, Ireland

M. Felcini, M. Grunewald

INFN Sezione di Bari^a, Università di Bari^b, Politecnico di Bari^c, Bari, Italy

M. Abbrescia^{a,b}, R. Aly^{a,b,30}, C. Calabria^{a,b}, A. Colaleo^a, D. Creanza^{a,c}, L. Cristella^{a,b}, N. De Filippis^{a,c}, M. De Palma^{a,b}, A. Di Florio^{a,b}, L. Fiore^a, A. Gelmi^{a,b}, G. Iaselli^{a,c}, M. Ince^{a,b}, S. Lezki^{a,b}, G. Maggi^{a,c}, M. Maggi^a, G. Miniello^{a,b}, S. My^{a,b}, S. Nuzzo^{a,b}, A. Pompili^{a,b}, G. Pugliese^{a,c}, R. Radogna^a, A. Ranieri^a, G. Selvaggi^{a,b}, L. Silvestris^a, R. Venditti^a, P. Verwilligen^a

INFN Sezione di Bologna^a, Università di Bologna^b, Bologna, Italy

G. Abbiendi^a, C. Battilana^{a,b}, D. Bonacorsi^{a,b}, L. Borgonovi^{a,b}, S. Braibant-Giacomelli^{a,b}, R. Campanini^{a,b}, P. Capiluppi^{a,b}, A. Castro^{a,b}, F.R. Cavallo^a, C. Ciocca^a, G. Codispoti^{a,b},

M. Cuffiani^{a,b}, G.M. Dallavalle^a, F. Fabbri^a, A. Fanfani^{a,b}, E. Fontanesi, P. Giacomelli^a, C. Grandi^a, L. Guiducci^{a,b}, F. Iemmi^{a,b}, S. Lo Meo^{a,31}, S. Marcellini^a, G. Masetti^a, F.L. Navarria^{a,b}, A. Perrotta^a, F. Primavera^{a,b}, A.M. Rossi^{a,b}, T. Rovelli^{a,b}, G.P. Siroli^{a,b}, N. Tosi^a

INFN Sezione di Catania^a, Università di Catania^b, Catania, Italy

S. Albergo^{a,b,32}, S. Costa^{a,b}, A. Di Mattia^a, R. Potenza^{a,b}, A. Tricomi^{a,b,32}, C. Tuve^{a,b}

INFN Sezione di Firenze^a, Università di Firenze^b, Firenze, Italy

G. Barbagli^a, R. Ceccarelli, K. Chatterjee^{a,b}, V. Ciulli^{a,b}, C. Civinini^a, R. D'Alessandro^{a,b}, E. Focardi^{a,b}, G. Latino, P. Lenzi^{a,b}, M. Meschini^a, S. Paoletti^a, G. Sguazzoni^a, D. Strom^a, L. Viliani^a

INFN Laboratori Nazionali di Frascati, Frascati, Italy

L. Benussi, S. Bianco, D. Piccolo

INFN Sezione di Genova^a, Università di Genova^b, Genova, Italy

M. Bozzo^{a,b}, F. Ferro^a, R. Mulargia^{a,b}, E. Robutti^a, S. Tosi^{a,b}

INFN Sezione di Milano-Bicocca^a, Università di Milano-Bicocca^b, Milano, Italy

A. Benaglia^a, A. Beschi^{a,b}, F. Brivio^{a,b}, V. Ciriolo^{a,b,18}, S. Di Guida^{a,b,18}, M.E. Dinardo^{a,b}, P. Dini^a, S. Fiorendi^{a,b}, S. Gennai^a, A. Ghezzi^{a,b}, P. Govoni^{a,b}, L. Guzzi^{a,b}, M. Malberti^a, S. Malvezzi^a, D. Menasce^a, F. Monti^{a,b}, L. Moroni^a, G. Ortona^{a,b}, M. Paganoni^{a,b}, D. Pedrini^a, S. Ragazzi^{a,b}, T. Tabarelli de Fatis^{a,b}, D. Zuolo^{a,b}

INFN Sezione di Napoli^a, Università di Napoli 'Federico II'^b, Napoli, Italy, Università della Basilicata^c, Potenza, Italy, Università G. Marconi^d, Roma, Italy

S. Buontempo^a, N. Cavallo^{a,c}, A. De Iorio^{a,b}, A. Di Crescenzo^{a,b}, F. Fabozzi^{a,c}, F. Fienga^a, G. Galati^a, A.O.M. Iorio^{a,b}, L. Lista^{a,b}, S. Meola^{a,d,18}, P. Paolucci^{a,18}, B. Rossi^a, C. Sciacca^{a,b}, E. Voevodina^{a,b}

INFN Sezione di Padova^a, Università di Padova^b, Padova, Italy, Università di Trento^c, Trento, Italy

P. Azzi^a, N. Bacchetta^a, D. Bisello^{a,b}, A. Boletti^{a,b}, A. Bragagnolo, R. Carlin^{a,b}, P. Checchia^a, P. De Castro Manzano^a, T. Dorigo^a, U. Dosselli^a, F. Gasparini^{a,b}, U. Gasparini^{a,b}, A. Gozzelino^a, S.Y. Hoh, P. Lujan, M. Margoni^{a,b}, A.T. Meneguzzo^{a,b}, J. Pazzini^{a,b}, M. Presilla^b, P. Ronchese^{a,b}, R. Rossin^{a,b}, F. Simonetto^{a,b}, A. Tiko, M. Tosi^{a,b}, M. Zanetti^{a,b}, P. Zotto^{a,b}, G. Zumerle^{a,b}

INFN Sezione di Pavia^a, Università di Pavia^b, Pavia, Italy

A. Braghieri^a, P. Montagna^{a,b}, S.P. Ratti^{a,b}, V. Re^a, M. Ressegotti^{a,b}, C. Riccardi^{a,b}, P. Salvini^a, I. Vai^{a,b}, P. Vitulo^{a,b}

INFN Sezione di Perugia^a, Università di Perugia^b, Perugia, Italy

M. Biasini^{a,b}, G.M. Bilei^a, C. Cecchi^{a,b}, D. Ciangottini^{a,b}, L. Fanò^{a,b}, P. Lariccia^{a,b}, R. Leonardi^{a,b}, E. Manoni^a, G. Mantovani^{a,b}, V. Mariani^{a,b}, M. Menichelli^a, A. Rossi^{a,b}, A. Santocchia^{a,b}, D. Spiga^a

**INFN Sezione di Pisa^a, Università di Pisa^b, Scuola Normale Superiore di Pisa^c,
Pisa, Italy**

K. Androsova^a, P. Azzurri^a, G. Bagliesi^a, V. Bertacchi^{a,c}, L. Bianchini^a, T. Boccali^a,
R. Castaldi^a, M.A. Ciocci^{a,b}, R. Dell’Orso^a, G. Fedi^a, L. Giannini^{a,c}, A. Giassi^a,
M.T. Grippo^a, F. Ligabue^{a,c}, E. Manca^{a,c}, G. Mandorli^{a,c}, A. Messineo^{a,b}, F. Palla^a,
A. Rizzi^{a,b}, G. Rolandi³³, S. Roy Chowdhury, A. Scribano^a, P. Spagnolo^a, R. Tenchini^a,
G. Tonelli^{a,b}, N. Turini, A. Venturi^a, P.G. Verdini^a

INFN Sezione di Roma^a, Sapienza Università di Roma^b, Rome, Italy

F. Cavallari^a, M. Cipriani^{a,b}, D. Del Re^{a,b}, E. Di Marco^{a,b}, M. Diemoz^a, E. Longo^{a,b},
B. Marzocchi^{a,b}, P. Meridiani^a, G. Organtini^{a,b}, F. Pandolfi^a, R. Paramatti^{a,b},
C. Quaranta^{a,b}, S. Rahatlou^{a,b}, C. Rovelli^a, F. Santanastasio^{a,b}, L. Soffi^{a,b}

**INFN Sezione di Torino^a, Università di Torino^b, Torino, Italy, Università del
Piemonte Orientale^c, Novara, Italy**

N. Amapane^{a,b}, R. Arcidiacono^{a,c}, S. Argiro^{a,b}, M. Arneodo^{a,c}, N. Bartosik^a, R. Bellan^{a,b},
C. Biino^a, A. Cappati^{a,b}, N. Cartiglia^a, S. Cometti^a, M. Costa^{a,b}, R. Covarelli^{a,b},
N. Demaria^a, B. Kiani^{a,b}, C. Mariotti^a, S. Maselli^a, E. Migliore^{a,b}, V. Monaco^{a,b},
E. Monteil^{a,b}, M. Monteno^a, M.M. Obertino^{a,b}, L. Pacher^{a,b}, N. Pastrone^a, M. Pelliccioni^a,
G.L. Pinna Angioni^{a,b}, A. Romero^{a,b}, M. Ruspa^{a,c}, R. Sacchi^{a,b}, R. Salvatico^{a,b}, V. Sola^a,
A. Solano^{a,b}, D. Soldi^{a,b}, A. Staiano^a

INFN Sezione di Trieste^a, Università di Trieste^b, Trieste, Italy

S. Belforte^a, V. Candelise^{a,b}, M. Casarsa^a, F. Cossutti^a, A. Da Rold^{a,b}, G. Della Ricca^{a,b},
F. Vazzoler^{a,b}, A. Zanetti^a

Kyungpook National University, Daegu, Korea

B. Kim, D.H. Kim, G.N. Kim, M.S. Kim, J. Lee, S.W. Lee, C.S. Moon, Y.D. Oh, S.I. Pak,
S. Sekmen, D.C. Son, Y.C. Yang

**Chonnam National University, Institute for Universe and Elementary Particles,
Kwangju, Korea**

H. Kim, D.H. Moon, G. Oh

Hanyang University, Seoul, Korea

B. Francois, T.J. Kim, J. Park

Korea University, Seoul, Korea

S. Cho, S. Choi, Y. Go, D. Gyun, S. Ha, B. Hong, K. Lee, K.S. Lee, J. Lim, J. Park,
S.K. Park, Y. Roh

Kyung Hee University, Department of Physics

J. Goh

Sejong University, Seoul, Korea

H.S. Kim

Seoul National University, Seoul, Korea

J. Almond, J.H. Bhyun, J. Choi, S. Jeon, J. Kim, J.S. Kim, H. Lee, K. Lee, S. Lee, K. Nam, M. Oh, S.B. Oh, B.C. Radburn-Smith, U.K. Yang, H.D. Yoo, I. Yoon, G.B. Yu

University of Seoul, Seoul, Korea

D. Jeon, H. Kim, J.H. Kim, J.S.H. Lee, I.C. Park, I. Watson

Sungkyunkwan University, Suwon, Korea

Y. Choi, C. Hwang, Y. Jeong, J. Lee, Y. Lee, I. Yu

Riga Technical University, Riga, Latvia

V. Veckalns³⁴

Vilnius University, Vilnius, Lithuania

V. Dudenas, A. Juodagalvis, G. Tamulaitis, J. Vaitkus

National Centre for Particle Physics, Universiti Malaya, Kuala Lumpur, Malaysia

Z.A. Ibrahim, F. Mohamad Idris³⁵, W.A.T. Wan Abdullah, M.N. Yusli, Z. Zolkapli

Universidad de Sonora (UNISON), Hermosillo, Mexico

J.F. Benitez, A. Castaneda Hernandez, J.A. Murillo Quijada, L. Valencia Palomo

Centro de Investigacion y de Estudios Avanzados del IPN, Mexico City, Mexico

H. Castilla-Valdez, E. De La Cruz-Burelo, I. Heredia-De La Cruz³⁶, R. Lopez-Fernandez, A. Sanchez-Hernandez

Universidad Iberoamericana, Mexico City, Mexico

S. Carrillo Moreno, C. Oropeza Barrera, M. Ramirez-Garcia, F. Vazquez Valencia

Benemerita Universidad Autonoma de Puebla, Puebla, Mexico

J. Eysermans, I. Pedraza, H.A. Salazar Ibarguen, C. Uribe Estrada

Universidad Autónoma de San Luis Potosí, San Luis Potosí, Mexico

A. Morelos Pineda

University of Montenegro, Podgorica, Montenegro

N. Raicevic

University of Auckland, Auckland, New Zealand

D. Krofcheck

University of Canterbury, Christchurch, New Zealand

S. Bheesette, P.H. Butler

National Centre for Physics, Quaid-I-Azam University, Islamabad, Pakistan

A. Ahmad, M. Ahmad, Q. Hassan, H.R. Hoorani, W.A. Khan, M.A. Shah, M. Shoaib, M. Waqas

AGH University of Science and Technology Faculty of Computer Science, Electronics and Telecommunications, Krakow, Poland

V. Avati, L. Grzanka, M. Malawski

National Centre for Nuclear Research, Swierk, Poland

H. Bialkowska, M. Bluj, B. Boimska, M. Górski, M. Kazana, M. Szleper, P. Zalewski

Institute of Experimental Physics, Faculty of Physics, University of Warsaw, Warsaw, Poland

K. Bunkowski, A. Byszuk³⁷, K. Doroba, A. Kalinowski, M. Konecki, J. Krolikowski, M. Misiura, M. Olszewski, A. Pyskir, M. Walczak

Laboratório de Instrumentação e Física Experimental de Partículas, Lisboa, Portugal

M. Araujo, P. Bargassa, D. Bastos, A. Di Francesco, P. Faccioli, B. Galinhas, M. Gallinaro, J. Hollar, N. Leonardo, J. Seixas, K. Shchelina, G. Strong, O. Toldaiev, J. Varela

Joint Institute for Nuclear Research, Dubna, Russia

S. Afanasiev, P. Bunin, M. Gavrilenko, I. Golutvin, I. Gorbunov, A. Kamenev, V. Karjavine, A. Lanev, A. Malakhov, V. Matveev^{38,39}, P. Moisezenz, V. Palichik, V. Perelygin, M. Savina, S. Shmatov, S. Shulha, N. Skatchkov, V. Smirnov, N. Voytishin, A. Zarubin

Petersburg Nuclear Physics Institute, Gatchina (St. Petersburg), Russia

L. Chtchipounov, V. Golovtsov, Y. Ivanov, V. Kim⁴⁰, E. Kuznetsova⁴¹, P. Levchenko, V. Murzin, V. Oreshkin, I. Smirnov, D. Sosnov, V. Sulimov, L. Uvarov, A. Vorobyev

Institute for Nuclear Research, Moscow, Russia

Yu. Andreev, A. Dermenev, S. Gninenko, N. Golubev, A. Karneyeu, M. Kirsanov, N. Krasnikov, A. Pashenkov, D. Tlisov, A. Toropin

Institute for Theoretical and Experimental Physics named by A.I. Alikhanov of NRC ‘Kurchatov Institute’, Moscow, Russia

V. Epshteyn, V. Gavrilov, N. Lychkovskaya, A. Nikitenko⁴², V. Popov, I. Pozdnyakov, G. Safronov, A. Spiridonov, A. Stepenov, M. Toms, E. Vlasov, A. Zhokin

Moscow Institute of Physics and Technology, Moscow, Russia

T. Aushev

National Research Nuclear University ‘Moscow Engineering Physics Institute’ (MEPhI), Moscow, Russia

M. Chadeeva⁴³, P. Parygin, D. Philippov, E. Popova, V. Rusinov

P.N. Lebedev Physical Institute, Moscow, Russia

V. Andreev, M. Azarkin, I. Dremin, M. Kirakosyan, A. Terkulov

Skobeltsyn Institute of Nuclear Physics, Lomonosov Moscow State University, Moscow, Russia

A. Belyaev, E. Boos, V. Bunichev, M. Dubinin⁴⁴, L. Dudko, A. Gribushin, V. Klyukhin, O. Kodolova, I. Lokhtin, S. Obraztsov, M. Perfilov, S. Petrushanko, V. Savrin

Novosibirsk State University (NSU), Novosibirsk, Russia

A. Barnyakov⁴⁵, V. Blinov⁴⁵, T. Dimova⁴⁵, L. Kardapoltsev⁴⁵, Y. Skovpen⁴⁵

Institute for High Energy Physics of National Research Centre ‘Kurchatov Institute’, Protvino, Russia

I. Azhgirey, I. Bayshev, S. Bitioukov, V. Kachanov, D. Konstantinov, P. Mandrik, V. Petrov, R. Ryutin, S. Slabospitskii, A. Sobol, S. Troshin, N. Tyurin, A. Uzunian, A. Volkov

National Research Tomsk Polytechnic University, Tomsk, Russia

A. Babaev, A. Iuzhakov, V. Okhotnikov

Tomsk State University, Tomsk, Russia

V. Borchsh, V. Ivanchenko, E. Tcherniaev

University of Belgrade: Faculty of Physics and VINCA Institute of Nuclear Sciences

P. Adzic⁴⁶, P. Cirkovic, D. Devetak, M. Dordevic, P. Milenovic, J. Milosevic, M. Stojanovic

Centro de Investigaciones Energéticas Medioambientales y Tecnológicas (CIEMAT), Madrid, Spain

M. Aguilar-Benitez, J. Alcaraz Maestre, A. Álvarez Fernández, I. Bachiller, M. Barrio Luna, J.A. Brochero Cifuentes, C.A. Carrillo Montoya, M. Cepeda, M. Cerrada, N. Colino, B. De La Cruz, A. Delgado Peris, C. Fernandez Bedoya, J.P. Fernández Ramos, J. Flix, M.C. Fouz, O. Gonzalez Lopez, S. Goy Lopez, J.M. Hernandez, M.I. Josa, D. Moran, Á. Navarro Tobar, A. Pérez-Calero Yzquierdo, J. Puerta Pelayo, I. Redondo, L. Romero, S. Sánchez Navas, M.S. Soares, A. Triossi, C. Willmott

Universidad Autónoma de Madrid, Madrid, Spain

C. Albajar, J.F. de Trocóniz

Universidad de Oviedo, Instituto Universitario de Ciencias y Tecnologías Espaciales de Asturias (ICTEA), Oviedo, Spain

B. Alvarez Gonzalez, J. Cuevas, C. Erice, J. Fernandez Menendez, S. Folgueras, I. Gonzalez Caballero, J.R. González Fernández, E. Palencia Cortezon, V. Rodríguez Bouza, S. Sanchez Cruz

Instituto de Física de Cantabria (IFCA), CSIC-Universidad de Cantabria, Santander, Spain

I.J. Cabrillo, A. Calderon, B. Chazin Quero, J. Duarte Campderros, M. Fernandez, P.J. Fernández Manteca, A. García Alonso, G. Gomez, C. Martinez Rivero, P. Martinez Ruiz del Arbol, F. Matorras, J. Piedra Gomez, C. Prieels, T. Rodrigo, A. Ruiz-Jimeno, L. Russo⁴⁷, L. Scodellaro, N. Trevisani, I. Vila, J.M. Vizán García

University of Colombo, Colombo, Sri Lanka

K. Malagalage

University of Ruhuna, Department of Physics, Matara, Sri Lanka

W.G.D. Dharmaratna, N. Wickramage

CERN, European Organization for Nuclear Research, Geneva, Switzerland

D. Abbaneo, B. Akgun, E. Auffray, G. Auzinger, J. Baechler, P. Baillon, A.H. Ball, D. Barney, J. Bendavid, M. Bianco, A. Bocci, E. Bossini, C. Botta, E. Brondolin, T. Camporesi, A. Caratelli, G. Cerminara, E. Chapon, G. Cucciati, D. d’Enterria, A. Dabrowski, N. Daci, V. Daponte, A. David, O. Davignon, A. De Roeck, N. Deelen, M. Deile, M. Dobson, M. Dünser, N. Dupont, A. Elliott-Peisert, F. Fallavollita⁴⁸, D. Fasanella, G. Franzoni, J. Fulcher, W. Funk, S. Giani, D. Gigi, A. Gilbert, K. Gill, F. Glege, M. Gruchala, M. Guilhaud, D. Gulhan, J. Hegeman, C. Heidegger, Y. Iiyama, V. Innocente, P. Janot, O. Karacheban²¹, J. Kaspar, J. Kieseler, M. Krammer¹, C. Lange, P. Lecoq, C. Lourenço, L. Malgeri, M. Mannelli, A. Massironi, F. Meijers, J.A. Merlin, S. Mersi, E. Meschi, F. Moortgat, M. Mulders, J. Ngadiuba, S. Nourbakhsh, S. Orfanelli, L. Orsini, F. Pantaleo¹⁸, L. Pape, E. Perez, M. Peruzzi, A. Petrilli, G. Petrucciani, A. Pfeiffer, M. Pierini, F.M. Pitters, D. Rabadý, A. Racz, M. Rovere, H. Sakulin, C. Schäfer, C. Schwick, M. Selvaggi, A. Sharma, P. Silva, W. Snoeys, P. Sphicas⁴⁹, J. Steggemann, V.R. Tavolaro, D. Treille, A. Tsiro, A. Vartak, M. Verzetti, W.D. Zeuner

Paul Scherrer Institut, Villigen, Switzerland

L. Caminada⁵⁰, K. Deiters, W. Erdmann, R. Horisberger, Q. Ingram, H.C. Kaestli, D. Kotlinski, U. Langenegger, T. Rohe, S.A. Wiederkehr

ETH Zurich — Institute for Particle Physics and Astrophysics (IPA), Zurich, Switzerland

M. Backhaus, P. Berger, N. Chernyavskaya, G. Dissertori, M. Dittmar, M. Donegà, C. Dorfer, T.A. Gómez Espinosa, C. Grab, D. Hits, T. Klijnsma, W. Lustermann, R.A. Manzoni, M. Marionneau, M.T. Meinhard, F. Micheli, P. Musella, F. Nessi-Tedaldi, F. Pauss, G. Perrin, L. Perrozzi, S. Pigazzini, M. Reichmann, C. Reissel, T. Reitenspiess, D. Ruini, D.A. Sanz Becerra, M. Schönenberger, L. Shchutska, M.L. Vesterbacka Olsson, R. Wallny, D.H. Zhu

Universität Zürich, Zurich, Switzerland

T.K. Aarrestad, C. Amsler⁵¹, D. Brzhechko, M.F. Canelli, A. De Cosa, R. Del Burgo, S. Donato, B. Kilminster, S. Leontsinis, V.M. Mikuni, I. Neutelings, G. Rauco, P. Robmann, D. Salerno, K. Schweiger, C. Seitz, Y. Takahashi, S. Wertz, A. Zucchetta

National Central University, Chung-Li, Taiwan

T.H. Doan, C.M. Kuo, W. Lin, A. Roy, S.S. Yu

National Taiwan University (NTU), Taipei, Taiwan

P. Chang, Y. Chao, K.F. Chen, P.H. Chen, W.-S. Hou, Y.y. Li, R.-S. Lu, E. Paganis, A. Psallidas, A. Steen

Chulalongkorn University, Faculty of Science, Department of Physics, Bangkok, Thailand

B. Asavapibhop, C. Asawatangtrakuldee, N. Srimanobhas, N. Suwonjandee

Çukurova University, Physics Department, Science and Art Faculty, Adana, Turkey

A. Bat, F. Boran, S. Cerci⁵², S. Damarseckin⁵³, Z.S. Demiroglu, F. Dolek, C. Dozen, I. Dumanoglu, G. Gokbulut, EmineGurpinar Guler⁵⁴, Y. Guler, I. Hos⁵⁵, C. Isik, E.E. Kangal⁵⁶, O. Kara, A. Kayis Topaksu, U. Kiminsu, M. Oglakci, G. Onengut, K. Ozdemir⁵⁷, S. Ozturk⁵⁸, A.E. Simsek, D. Sunar Cerci⁵², U.G. Tok, S. Turkcapar, I.S. Zorbakir, C. Zorbilmez

Middle East Technical University, Physics Department, Ankara, Turkey

B. Isildak⁵⁹, G. Karapinar⁶⁰, M. Yalvac

Bogazici University, Istanbul, Turkey

I.O. Atakisi, E. Gülmez, M. Kaya⁶¹, O. Kaya⁶², B. Kaynak, Ö. Özçelik, S. Tekten, E.A. Yetkin⁶³

Istanbul Technical University, Istanbul, Turkey

A. Cakir, K. Cankocak, Y. Komurcu, S. Sen⁶⁴

Istanbul University, Istanbul, Turkey

S. Ozkorucuklu

Institute for Scintillation Materials of National Academy of Science of Ukraine, Kharkov, Ukraine

B. Grynyov

National Scientific Center, Kharkov Institute of Physics and Technology, Kharkov, Ukraine

L. Levchuk

University of Bristol, Bristol, United Kingdom

F. Ball, E. Bhal, S. Bologna, J.J. Brooke, D. Burns, E. Clement, D. Cussans, H. Flacher, J. Goldstein, G.P. Heath, H.F. Heath, L. Kreczko, S. Paramesvaran, B. Penning, T. Sakuma, S. Seif El Nasr-Storey, D. Smith, V.J. Smith, J. Taylor, A. Titterton

Rutherford Appleton Laboratory, Didcot, United Kingdom

K.W. Bell, A. Belyaev⁶⁵, C. Brew, R.M. Brown, D. Cieri, D.J.A. Cockerill, J.A. Coughlan, K. Harder, S. Harper, J. Linacre, K. Manolopoulos, D.M. Newbold, E. Olaiya, D. Petyt, T. Reis, T. Schuh, C.H. Shepherd-Themistocleous, A. Thea, I.R. Tomalin, T. Williams, W.J. Womersley

Imperial College, London, United Kingdom

R. Bainbridge, P. Bloch, J. Borg, S. Breeze, O. Buchmuller, A. Bundock, GurpreetSingh CHAHAL⁶⁶, D. Colling, P. Dauncey, G. Davies, M. Della Negra, R. Di Maria, P. Everaerts, G. Hall, G. Iles, T. James, M. Komm, C. Laner, L. Lyons, A.-M. Magnan, S. Malik, A. Martelli, V. Milosevic, J. Nash⁶⁷, V. Palladino, M. Pesaresi, D.M. Raymond, A. Richards, A. Rose, E. Scott, C. Seez, A. Shtipliyski, M. Stoye, T. Strebler, S. Summers, A. Tapper, K. Uchida, T. Virdee¹⁸, N. Wardle, D. Winterbottom, J. Wright, A.G. Zecchinelli, S.C. Zenz

Brunel University, Uxbridge, United Kingdom

J.E. Cole, P.R. Hobson, A. Khan, P. Kyberd, C.K. Mackay, A. Morton, I.D. Reid, L. Teodorescu, S. Zahid

Baylor University, Waco, U.S.A.

K. Call, J. Dittmann, K. Hatakeyama, C. Madrid, B. McMaster, N. Pastika, C. Smith

Catholic University of America, Washington, DC, U.S.A.

R. Bartek, A. Dominguez, R. Uniyal

The University of Alabama, Tuscaloosa, U.S.A.

A. Buccilli, S.I. Cooper, C. Henderson, P. Rumerio, C. West

Boston University, Boston, U.S.A.

D. Arcaro, T. Bose, Z. Demiragli, D. Gastler, S. Girgis, D. Pinna, C. Richardson, J. Rohlf, D. Sperka, I. Suarez, L. Sulak, D. Zou

Brown University, Providence, U.S.A.

G. Benelli, B. Burkle, X. Coubez, D. Cutts, Y.t. Duh, M. Hadley, J. Hakala, U. Heintz, J.M. Hogan⁶⁸, K.H.M. Kwok, E. Laird, G. Landsberg, J. Lee, Z. Mao, M. Narain, S. Sagir⁶⁹, R. Syarif, E. Usai, D. Yu

University of California, Davis, Davis, U.S.A.

R. Band, C. Brainerd, R. Breedon, M. Calderon De La Barca Sanchez, M. Chertok, J. Conway, R. Conway, P.T. Cox, R. Erbacher, C. Flores, G. Funk, F. Jensen, W. Ko, O. Kukral, R. Lander, M. Mulhearn, D. Pellett, J. Pilot, M. Shi, D. Stolp, D. Taylor, K. Tos, M. Tripathi, Z. Wang, F. Zhang

University of California, Los Angeles, U.S.A.

M. Bachtis, C. Bravo, R. Cousins, A. Dasgupta, A. Florent, J. Hauser, M. Ignatenko, N. Mccoll, W.A. Nash, S. Regnard, D. Saltzberg, C. Schnaible, B. Stone, V. Valuev

University of California, Riverside, Riverside, U.S.A.

K. Burt, R. Clare, J.W. Gary, S.M.A. Ghiasi Shirazi, G. Hanson, G. Karapostoli, E. Kennedy, O.R. Long, M. Olmedo Negrete, M.I. Paneva, W. Si, L. Wang, H. Wei, S. Wimpenny, B.R. Yates, Y. Zhang

University of California, San Diego, La Jolla, U.S.A.

J.G. Branson, P. Chang, S. Cittolin, M. Derdzinski, R. Gerosa, D. Gilbert, B. Hashemi, D. Klein, V. Krutelyov, J. Letts, M. Masciovecchio, S. May, S. Padhi, M. Pieri, V. Sharma, M. Tadel, F. Würthwein, A. Yagil, G. Zevi Della Porta

University of California, Santa Barbara — Department of Physics, Santa Barbara, U.S.A.

N. Amin, R. Bhandari, C. Campagnari, M. Citron, V. Dutta, M. Franco Sevilla, L. Gouskos, J. Incandela, B. Marsh, H. Mei, A. Ovcharova, H. Qu, J. Richman, U. Sarica, D. Stuart, S. Wang, J. Yoo

California Institute of Technology, Pasadena, U.S.A.

D. Anderson, A. Bornheim, O. Cerri, I. Dutta, J.M. Lawhorn, N. Lu, J. Mao, H.B. Newman, T.Q. Nguyen, J. Pata, M. Spiropulu, J.R. Vlimant, S. Xie, Z. Zhang, R.Y. Zhu

Carnegie Mellon University, Pittsburgh, U.S.A.

M.B. Andrews, T. Ferguson, T. Mudholkar, M. Paulini, M. Sun, I. Vorobiev, M. Weinberg

University of Colorado Boulder, Boulder, U.S.A.

J.P. Cumalat, W.T. Ford, A. Johnson, E. MacDonald, T. Mulholland, R. Patel, A. Perloff, K. Stenson, K.A. Ulmer, S.R. Wagner

Cornell University, Ithaca, U.S.A.

J. Alexander, J. Chaves, Y. Cheng, J. Chu, A. Datta, A. Frankenthal, K. McDermott, N. Mirman, J.R. Patterson, D. Quach, A. Rinkevicius⁷⁰, A. Ryd, S.M. Tan, Z. Tao, J. Thom, P. Wittich, M. Zientek

Fermi National Accelerator Laboratory, Batavia, U.S.A.

S. Abdullin, M. Albrow, M. Alyari, G. Apollinari, A. Apresyan, A. Apyan, S. Banerjee, L.A.T. Bauerdick, A. Beretvas, J. Berryhill, P.C. Bhat, K. Burkett, J.N. Butler, A. Canepa, G.B. Cerati, H.W.K. Cheung, F. Chlebana, M. Cremonesi, J. Duarte, V.D. Elvira, J. Freeman, Z. Gecse, E. Gottschalk, L. Gray, D. Green, S. Grünendahl, O. Gutsche, AllisonReinsvold Hall, J. Hanlon, R.M. Harris, S. Hasegawa, R. Heller, J. Hirschauer, B. Jayatilaka, S. Jindariani, M. Johnson, U. Joshi, B. Klima, M.J. Kortelainen, B. Kreis, S. Lammel, J. Lewis, D. Lincoln, R. Lipton, M. Liu, T. Liu, J. Lykken, K. Maeshima, J.M. Marraffino, D. Mason, P. McBride, P. Merkel, S. Mrenna, S. Nahn, V. O'Dell, V. Papadimitriou, K. Pedro, C. Pena, G. Rakness, F. Ravera, L. Ristori, B. Schneider, E. Sexton-Kennedy, N. Smith, A. Soha, W.J. Spalding, L. Spiegel, S. Stoynev, J. Strait, N. Strobbe, L. Taylor, S. Tkaczyk, N.V. Tran, L. Uplegger, E.W. Vaandering, C. Vernieri, M. Verzocchi, R. Vidal, M. Wang, H.A. Weber

University of Florida, Gainesville, U.S.A.

D. Acosta, P. Avery, P. Bortignon, D. Bourilkov, A. Brinkerhoff, L. Cadamuro, A. Carnes, V. Cherepanov, D. Curry, F. Errico, R.D. Field, S.V. Gleyzer, B.M. Joshi, M. Kim, J. Konigsberg, A. Korytov, K.H. Lo, P. Ma, K. Matchev, N. Menendez, G. Mitselmakher, D. Rosenzweig, K. Shi, J. Wang, S. Wang, X. Zuo

Florida International University, Miami, U.S.A.

Y.R. Joshi

Florida State University, Tallahassee, U.S.A.

T. Adams, A. Askew, S. Hagopian, V. Hagopian, K.F. Johnson, R. Khurana, T. Kolberg, G. Martinez, T. Perry, H. Prosper, C. Schiber, R. Yohay, J. Zhang

Florida Institute of Technology, Melbourne, U.S.A.

M.M. Baarmand, V. Bhopatkar, M. Hohlmann, D. Noonan, M. Rahmani, M. Saunders, F. Yumiceva

University of Illinois at Chicago (UIC), Chicago, U.S.A.

M.R. Adams, L. Apanasevich, D. Berry, R.R. Betts, R. Cavanaugh, X. Chen, S. Dittmer, O. Evdokimov, C.E. Gerber, D.A. Hangal, D.J. Hofman, K. Jung, C. Mills, T. Roy, M.B. Tonjes, N. Varelas, H. Wang, X. Wang, Z. Wu

The University of Iowa, Iowa City, U.S.A.

M. Alhusseini, B. Bilki⁵⁴, W. Clarida, K. Dilsiz⁷¹, S. Durgut, R.P. Gandrajula, M. Haytmyradov, V. Khristenko, O.K. Köseyan, J.-P. Merlo, A. Mestvirishvili⁷², A. Moeller, J. Nachtman, H. Ogul⁷³, Y. Onel, F. Ozok⁷⁴, A. Penzo, C. Snyder, E. Tiras, J. Wetzel

Johns Hopkins University, Baltimore, U.S.A.

B. Blumenfeld, A. Cocoros, N. Eminizer, D. Fehling, L. Feng, A.V. Gritsan, W.T. Hung, P. Maksimovic, J. Roskes, M. Swartz, M. Xiao

The University of Kansas, Lawrence, U.S.A.

C. Baldenegro Barrera, P. Baringer, A. Bean, S. Boren, J. Bowen, A. Bylinkin, T. Isidori, S. Khalil, J. King, G. Krintiras, A. Kropivnitskaya, C. Lindsey, D. Majumder, W. Mcbrayer, N. Minafra, M. Murray, C. Rogan, C. Royon, S. Sanders, E. Schmitz, J.D. Tapia Takaki, Q. Wang, J. Williams, G. Wilson

Kansas State University, Manhattan, U.S.A.

S. Duric, A. Ivanov, K. Kaadze, D. Kim, Y. Maravin, D.R. Mendis, T. Mitchell, A. Modak, A. Mohammadi

Lawrence Livermore National Laboratory, Livermore, U.S.A.

F. Rebassoo, D. Wright

University of Maryland, College Park, U.S.A.

A. Baden, O. Baron, A. Belloni, S.C. Eno, Y. Feng, N.J. Hadley, S. Jabeen, G.Y. Jeng, R.G. Kellogg, J. Kunkle, A.C. Mignerey, S. Nabili, F. Ricci-Tam, M. Seidel, Y.H. Shin, A. Skuja, S.C. Tonwar, K. Wong

Massachusetts Institute of Technology, Cambridge, U.S.A.

D. Abercrombie, B. Allen, A. Baty, R. Bi, S. Brandt, W. Busza, I.A. Cali, M. D’Alfonso, G. Gomez Ceballos, M. Goncharov, P. Harris, D. Hsu, M. Hu, M. Klute, D. Kovalskyi, Y.-J. Lee, P.D. Luckey, B. Maier, A.C. Marini, C. McGinn, C. Mironov, S. Narayanan, X. Niu, C. Paus, D. Rankin, C. Roland, G. Roland, Z. Shi, G.S.F. Stephens, K. Sumorok, K. Tatar, D. Velicanu, J. Wang, T.W. Wang, B. Wyslouch

University of Minnesota, Minneapolis, U.S.A.

A.C. Benvenuti[†], R.M. Chatterjee, A. Evans, S. Guts, P. Hansen, J. Hiltbrand, Sh. Jain, S. Kalafut, Y. Kubota, Z. Lesko, J. Mans, R. Rusack, M.A. Wadud

University of Mississippi, Oxford, U.S.A.

J.G. Acosta, S. Oliveros

University of Nebraska-Lincoln, Lincoln, U.S.A.

K. Bloom, D.R. Claes, C. Fangmeier, L. Finco, F. Golf, R. Gonzalez Suarez, R. Kamalieddin, I. Kravchenko, J.E. Siado, G.R. Snow, B. Stieger

State University of New York at Buffalo, Buffalo, U.S.A.

G. Agarwal, C. Harrington, I. Iashvili, A. Kharchilava, C. Mclean, D. Nguyen, A. Parker, J. Pekkanen, S. Rappoccio, B. Roozbahani

Northeastern University, Boston, U.S.A.

G. Alverson, E. Barberis, C. Freer, Y. Haddad, A. Hortiangtham, G. Madigan, D.M. Morse, T. Orimoto, L. Skinnari, A. Tishelman-Charny, T. Wamorkar, B. Wang, A. Wisecarver, D. Wood

Northwestern University, Evanston, U.S.A.

S. Bhattacharya, J. Bueghly, T. Gunter, K.A. Hahn, N. Odell, M.H. Schmitt, K. Sung, M. Trovato, M. Velasco

University of Notre Dame, Notre Dame, U.S.A.

R. Bucci, N. Dev, R. Goldouzian, M. Hildreth, K. Hurtado Anampa, C. Jessop, D.J. Karmgard, K. Lannon, W. Li, N. Loukas, N. Marinelli, I. Mcalister, F. Meng, C. Mueller, Y. Musienko³⁸, M. Planer, R. Ruchti, P. Siddireddy, G. Smith, S. Taroni, M. Wayne, A. Wightman, M. Wolf, A. Woodard

The Ohio State University, Columbus, U.S.A.

J. Alimena, B. Bylsma, L.S. Durkin, S. Flowers, B. Francis, C. Hill, W. Ji, A. Lefeld, T.Y. Ling, B.L. Winer

Princeton University, Princeton, U.S.A.

S. Cooperstein, G. Dezoort, P. Elmer, J. Hardenbrook, N. Haubrich, S. Higginbotham, A. Kalogeropoulos, S. Kwan, D. Lange, M.T. Lucchini, J. Luo, D. Marlow, K. Mei, I. Ojalvo, J. Olsen, C. Palmer, P. Piroué, J. Salfeld-Nebgen, D. Stickland, C. Tully, Z. Wang

University of Puerto Rico, Mayaguez, U.S.A.

S. Malik, S. Norberg

Purdue University, West Lafayette, U.S.A.

A. Barker, V.E. Barnes, S. Das, L. Gutay, M. Jones, A.W. Jung, A. Khatiwada, B. Mahakud, D.H. Miller, G. Negro, N. Neumeister, C.C. Peng, S. Piperov, H. Qiu, J.F. Schulte, J. Sun, F. Wang, R. Xiao, W. Xie

Purdue University Northwest, Hammond, U.S.A.

T. Cheng, J. Dolen, N. Parashar

Rice University, Houston, U.S.A.

K.M. Ecklund, S. Freed, F.J.M. Geurts, M. Kilpatrick, Arun Kumar, W. Li, B.P. Padley, R. Redjimi, J. Roberts, J. Rorie, W. Shi, A.G. Stahl Leiton, Z. Tu, A. Zhang

University of Rochester, Rochester, U.S.A.

A. Bodek, P. de Barbaro, R. Demina, J.L. Dulemba, C. Fallon, T. Ferbel, M. Galanti, A. Garcia-Bellido, J. Han, O. Hindrichs, A. Khukhunaishvili, E. Ranken, P. Tan, R. Taus

Rutgers, The State University of New Jersey, Piscataway, U.S.A.

B. Chiarito, J.P. Chou, A. Gandrakota, Y. Gershtein, E. Halkiadakis, A. Hart, M. Heindl, E. Hughes, S. Kaplan, S. Kyriacou, I. Laflotte, A. Lath, R. Montalvo, K. Nash, M. Os-
herson, H. Saka, S. Salur, S. Schnetzer, D. Sheffield, S. Somalwar, R. Stone, S. Thomas,
P. Thomassen

University of Tennessee, Knoxville, U.S.A.

H. Acharya, A.G. Delannoy, J. Heideman, G. Riley, S. Spanier

Texas A&M University, College Station, U.S.A.

O. Bouhali⁷⁵, A. Celik, M. Dalchenko, M. De Mattia, A. Delgado, S. Dildick, R. Eusebi,
J. Gilmore, T. Huang, T. Kamon⁷⁶, S. Luo, D. Marley, R. Mueller, D. Overton, L. Perniè,
D. Rathjens, A. Safonov

Texas Tech University, Lubbock, U.S.A.

N. Akchurin, J. Damgov, F. De Guio, S. Kunori, K. Lamichhane, S.W. Lee, T. Mengke,
S. Muthumuni, T. Peltola, S. Undleeb, I. Volobouev, Z. Wang, A. Whitbeck

Vanderbilt University, Nashville, U.S.A.

S. Greene, A. Gurrola, R. Janjam, W. Johns, C. Maguire, A. Melo, H. Ni, K. Padeken,
F. Romeo, P. Sheldon, S. Tuo, J. Velkovska, M. Verweij

University of Virginia, Charlottesville, U.S.A.

M.W. Arenton, P. Barria, B. Cox, G. Cummings, R. Hirosky, M. Joyce, A. Ledovskoy,
C. Neu, B. Tannenwald, Y. Wang, E. Wolfe, F. Xia

Wayne State University, Detroit, U.S.A.

R. Harr, P.E. Karchin, N. Poudyal, J. Sturdy, P. Thapa, S. Zaleski

University of Wisconsin — Madison, Madison, WI, U.S.A.

J. Buchanan, C. Caillol, D. Carlsmith, S. Dasu, I. De Bruyn, L. Dodd, F. Fiori, C. Galloni,
B. Gomer⁷⁷, H. He, M. Herndon, A. Hervé, U. Hussain, P. Klabbers, A. Lanaro,
A. Loeliger, K. Long, R. Loveless, J. Madhusudanan Sreekala, T. Ruggles, A. Savin,
V. Sharma, W.H. Smith, D. Teague, S. Trembath-reichert, N. Woods

†: Deceased

1: Also at Vienna University of Technology, Vienna, Austria

2: Also at IRFU, CEA, Université Paris-Saclay, Gif-sur-Yvette, France

3: Also at Universidade Estadual de Campinas, Campinas, Brazil

4: Also at Federal University of Rio Grande do Sul, Porto Alegre, Brazil

5: Also at UFMS, Nova Andradina, Brazil

6: Also at Universidade Federal de Pelotas, Pelotas, Brazil

7: Also at Université Libre de Bruxelles, Bruxelles, Belgium

8: Also at University of Chinese Academy of Sciences, Beijing, China

9: Also at Institute for Theoretical and Experimental Physics named by A.I. Alikhanov of NRC
‘Kurchatov Institute’, Moscow, Russia

10: Also at Joint Institute for Nuclear Research, Dubna, Russia

11: Also at Cairo University, Cairo, Egypt

- 12: Also at British University in Egypt, Cairo, Egypt
- 13: Now at Ain Shams University, Cairo, Egypt
- 14: Also at Purdue University, West Lafayette, U.S.A.
- 15: Also at Université de Haute Alsace, Mulhouse, France
- 16: Also at Tbilisi State University, Tbilisi, Georgia
- 17: Also at Erzincan Binali Yildirim University, Erzincan, Turkey
- 18: Also at CERN, European Organization for Nuclear Research, Geneva, Switzerland
- 19: Also at RWTH Aachen University, III. Physikalisches Institut A, Aachen, Germany
- 20: Also at University of Hamburg, Hamburg, Germany
- 21: Also at Brandenburg University of Technology, Cottbus, Germany
- 22: Also at Institute of Physics, University of Debrecen, Debrecen, Hungary, Debrecen, Hungary
- 23: Also at Institute of Nuclear Research ATOMKI, Debrecen, Hungary
- 24: Also at MTA-ELTE Lendület CMS Particle and Nuclear Physics Group, Eötvös Loránd University, Budapest, Hungary, Budapest, Hungary
- 25: Also at IIT Bhubaneswar, Bhubaneswar, India, Bhubaneswar, India
- 26: Also at Institute of Physics, Bhubaneswar, India
- 27: Also at Shoolini University, Solan, India
- 28: Also at University of Visva-Bharati, Santiniketan, India
- 29: Also at Isfahan University of Technology, Isfahan, Iran
- 30: Now at INFN Sezione di Bari^a, Università di Bari^b, Politecnico di Bari^c, Bari, Italy
- 31: Also at Italian National Agency for New Technologies, Energy and Sustainable Economic Development, Bologna, Italy
- 32: Also at Centro Siciliano di Fisica Nucleare e di Struttura Della Materia, Catania, Italy
- 33: Also at Scuola Normale e Sezione dell'INFN, Pisa, Italy
- 34: Also at Riga Technical University, Riga, Latvia, Riga, Latvia
- 35: Also at Malaysian Nuclear Agency, MOSTI, Kajang, Malaysia
- 36: Also at Consejo Nacional de Ciencia y Tecnología, Mexico City, Mexico
- 37: Also at Warsaw University of Technology, Institute of Electronic Systems, Warsaw, Poland
- 38: Also at Institute for Nuclear Research, Moscow, Russia
- 39: Now at National Research Nuclear University 'Moscow Engineering Physics Institute' (MEPhI), Moscow, Russia
- 40: Also at St. Petersburg State Polytechnical University, St. Petersburg, Russia
- 41: Also at University of Florida, Gainesville, U.S.A.
- 42: Also at Imperial College, London, United Kingdom
- 43: Also at P.N. Lebedev Physical Institute, Moscow, Russia
- 44: Also at California Institute of Technology, Pasadena, U.S.A.
- 45: Also at Budker Institute of Nuclear Physics, Novosibirsk, Russia
- 46: Also at Faculty of Physics, University of Belgrade, Belgrade, Serbia
- 47: Also at Università degli Studi di Siena, Siena, Italy
- 48: Also at INFN Sezione di Pavia^a, Università di Pavia^b, Pavia, Italy, Pavia, Italy
- 49: Also at National and Kapodistrian University of Athens, Athens, Greece
- 50: Also at Universität Zürich, Zurich, Switzerland
- 51: Also at Stefan Meyer Institute for Subatomic Physics, Vienna, Austria, Vienna, Austria
- 52: Also at Adiyaman University, Adiyaman, Turkey
- 53: Also at Şırnak University, Şırnak, Turkey
- 54: Also at Beykent University, Istanbul, Turkey, Istanbul, Turkey
- 55: Also at Istanbul Aydın University, Application and Research Center for Advanced Studies (App. & Res. Cent. for Advanced Studies), Istanbul, Turkey

- 56: Also at Mersin University, Mersin, Turkey
- 57: Also at Piri Reis University, Istanbul, Turkey
- 58: Also at Gaziosmanpasa University, Tokat, Turkey
- 59: Also at Ozyegin University, Istanbul, Turkey
- 60: Also at Izmir Institute of Technology, Izmir, Turkey
- 61: Also at Marmara University, Istanbul, Turkey
- 62: Also at Kafkas University, Kars, Turkey
- 63: Also at Istanbul Bilgi University, Istanbul, Turkey
- 64: Also at Hacettepe University, Ankara, Turkey
- 65: Also at School of Physics and Astronomy, University of Southampton, Southampton, United Kingdom
- 66: Also at IPPP Durham University, Durham, United Kingdom
- 67: Also at Monash University, Faculty of Science, Clayton, Australia
- 68: Also at Bethel University, St. Paul, Minneapolis, U.S.A., St. Paul, U.S.A.
- 69: Also at Karamanoğlu Mehmetbey University, Karaman, Turkey
- 70: Also at Vilnius University, Vilnius, Lithuania
- 71: Also at Bingol University, Bingol, Turkey
- 72: Also at Georgian Technical University, Tbilisi, Georgia
- 73: Also at Sinop University, Sinop, Turkey
- 74: Also at Mimar Sinan University, Istanbul, Istanbul, Turkey
- 75: Also at Texas A&M University at Qatar, Doha, Qatar
- 76: Also at Kyungpook National University, Daegu, Korea, Daegu, Korea
- 77: Also at University of Hyderabad, Hyderabad, India